Send Orders for Reprints to reprints@benthamscience.net

242 *Current Inorganic Chemistry,* 2013, *3,* 242-259

Modeling Transition Metal Complexes in the Framework of the Spin-Crossover Phenomenon: A DFT Perspective

Latévi Max Lawson Daku*

Département de chimie physique, Université de Genève, Quai E. Ansermet 30, CH-1211 Genève 4, Switzerland

Abstract: Using the study of the low-spin complex $[Fe(bpy)_3]^{2+}$ in the gas phase and in condensed phases as a guideline, we examine different aspects of the application of DFT to the study of transition metal complexes in the framework of spin crossover or related phenomena.

Keywords: Density functional theory, spin crossover, transition metal complexes.

1. INTRODUCTION

The electronic ground state of octahedral $3d^4 - 3d^7$ transition metal complexes is either the high-spin (HS) state, which is characterized by a maximum number of unpaired electrons in the $3d$ shell and thus by the maximum value of the total electronic spin *S*, or the low-spin (LS) state, which, with a maximum number of paired electrons in the d shell, is associated with the minimum value of *S*. Given that the LS $\rightarrow$ HS change of states involves the promotion of one or two electrons from the nonbonding t_{2g} to the antibonding e_g level, the metal-ligand bond length r will be larger in the HS state than in the LS state: $r_{HS} > r_{LS}$. The weakening of the metal-ligand bond translates into a higher vibrational density of states in the HS state, and, concomittantly, into a larger vibrational contribution $\mathcal{S}^{vib}$ to the entropy: $\Delta\mathcal{S}^{vib}_{HL} = \mathcal{S}^{vib}_{HS} - \mathcal{S}^{vib}_{LS} > 0$. Because of the higher degeneracy of the HS state, the electronic contribution $\mathcal{S}^{el}$ to the entropy is also larger in the HS state than in the LS state: $\Delta\mathcal{S}^{el}_{HL} = \mathcal{S}^{el}_{HS} - \mathcal{S}^{el}_{LS} > 0$. Consequently, the HS-LS entropy difference is positive: $\Delta\mathcal{S}_{HL} = \Delta\mathcal{S}^{el}_{HL} + \Delta\mathcal{S}^{vib}_{HL} > 0$. The HS-LS Gibbs free energy difference is given by:

$$\Delta\mathcal{G}_{HL}(T,P) = \Delta H_{HL}(T,P) - T\Delta\mathcal{S}_{HL}(T,P) \quad (1)$$

where ΔH_{HL} is the HS-LS enthalpy difference, and the dependence of the thermodynamic functions on temperature T and pressure P is made explicit. Given that $-T\Delta\mathcal{S}_{HL} < 0$, if the HS state is the quantum electronic ground state, that is, if the HS-LS zero-point energy difference $\Delta E^{\circ}_{HL} = E^{\circ}_{HS} - E^{\circ}_{LS}$ is negative ($\Delta E^{\circ}_{HL} \leq 0$), then the HS state remains the only noticeably populated state at all temperatures. Such complexes are termed *HS complexes*. If the LS state is the electronic ground sate ($\Delta E^{\circ}_{HL} > 0$), two situations can occur. If ΔE°_{HL} is far larger than the thermally accessible energies ($\Delta E^{\circ}_{HL} >> k_B T$), the complexes remain in their quantum mechanical LS ground state for all accessible temperatures, and the complexes are termed *LS complexes*. When ΔE°_{HL} is of the order of thermally accessible energies ($\Delta E^{\circ}_{HL} \sim k_B T$), one can observe the phenomenon of spin crossover, that is, the entropy-driven thermal depopulation of their electronic LS ground state in favor of the close-lying HS state. The phenomenon is accompanied by a change of the optical, magnetic and structural properties of the complexes. The LS $\leftrightarrows$ HS equilibrium can be influenced by external pressure [1]. Light irradiation can also be used to control the spin equilibrium [2]. *Spin-crossover complexes* and derived materials are therefore likely to be used in the design of optical devices for the storage and display of information at the molecular level. As such, they are the subject of numerous multidisciplinary studies [3-5].

The HS fraction γ_{HS} in a spin-crossover system can be obtained from spectroscopic or magnetization measurements. The knowledge of the transition curve $\gamma_{HS} = \gamma_{HS}(T,P)$ allows to determine the thermodynamics of spin crossover [6]. The HS-LS Gibbs free-energy difference is given by:

$$\Delta\mathcal{G}_{HL}(T,P) = -RT\log\left(\frac{\gamma_{HS}}{1-\gamma_{HS}}\right) \quad (2)$$

and the HS-LS enthaphy difference by

$$\Delta H_{HL}(T,P) = \Delta\mathcal{G}_{HL}(T,P) - T\left(\frac{\partial\Delta\mathcal{G}_{HL}}{\partial T}\right)_P \quad (3)$$

The ΔH_{HL} values usually reported and used as estimates of ΔE°_{HL} are for ambient pressure P_0 and the transition temperature $T_{1/2}$, which is the temperature at which $\gamma_{HS} = 1/2$. That is,

$$\Delta E^{\circ}_{HL} \approx \Delta H_{HL}(T_{1/2}, P_0) = T_{1/2}\Delta S_{HL}(T_{1/2}, P_0) \quad (4)$$

Although examples of spin crossover can be found for complexes of chromium, manganese, iron and cobalt in their common oxidation states [7, 8], the vast majority of spin-crossover complexes are hexacoordinated $3d^6$ iron(II) complexes with ligands providing a $[FeN_6]$ core. This probably follows from the fact that these complexes show the largest changes in their electronic properties and in their structures, and that the spin crossover transition can be accompanied by strong cooperative effects [6]. Iron(II)

*Address correspondence to this author at the Département de chimie physique, Université de Genève, Quai E. Ansermet 30, CH-1211 Genève 4, Switzerland; Tel: +41 22 379 6548; Fax: +41 22 379 6103;
E-mail: max.lawson@unige.ch

1877-945X/13 $58.00+.00

complexes are diamagnetic in the LS $^1A_{1g}(t_{2g}^6)$ state (S = 0) and paramagnetic in the HS $^5T_{2g}(t_{2g}^4 e_g^2)$ state (S = 2). Their electronic absorption properties change a lot with their spin state: the compounds are deeply colored in the LS state and tend to be weakly colored or even colorless in the HS state. The large structural changes in the $[FeN_6]$ complexes are associated with average LS and HS Fe-N distances of $r_{LS} \approx 2.0$ Å and $r_{HS} \approx 2.2$ Å, respectively, and follow from the fact that the LS $\rightarrow$ HS transition involves the promotion of two electrons from the nonbonding t_{2g} to the antibonding e_g level. For an iron(II) complex, ΔS_{HL} varies between 3 and 7 cm^{-1} K^{-1}, with an average value of 5 cm^{-1} K^{-1} [2]. Hence, for observing spin crossover in the temperature range from 50 to around 400 K, ΔE_{HL}° must be in the range 0-2000 cm^{-1} (Eq. (4)). The numerous manners in which the amine, imine, azole or pyridine ligands can be synthetically tailored to keep ΔE_{HL}° within the spin-crossover region largely contribute to the observed wealth of spin-crossover iron(II) complexes with a $[FeN_6]$ core. As discussed in details in Ref. [9], spin crossover is well understood on the basis of ligand field theoretical considerations, but the use of accurate computational methods is required to achieve an in-depth and quantitative understanding of the involved phenomena.

Density functional theory (DFT) in its Kohn-Sham (KS) formulation [10, 11] is an efficient approach to the elucidation of the electronic structure, which finds many successfull applications in quantum chemistry and in condensed-matter physics [12-15]. In DFT, the so-called exchange-correlation energy functional only needs to be appromixated. The search for accurate density functional approximations is a very active research area, wherein numerous functionals are regularly designed either non-empirically so as to satisfy as many exact theoretical constraints as possible, or by empirical fitting to accurate experimental or *ab initio* data. For detailed discussions of the density-functional approximation schemes, one can refer to Refs. [16-21], for instance. The application of DFT to the study of transition metal complexes in the framework of spin crossover have been pioneered by Bolvin [22] and by Paulsen and coworkers [23]. Since then, there has been in the field a tremendous number of investigations based on DFT. In this document, we try to give an overview which reflects the current state of the application of DFT to the modeling of transition metal complexes in the framework of spin crossover and related phenomena, using as a guideline three of our own studies on the complex $[Fe(bpy)_3]^{2+}$ (bpy = 2,2'-bipyridine). Although this complex is a LS complex and thus does not exhibit thermal spin crossover, it has received much attention because the HS state can be populated by photoexcitation like in spin-crossover complexes so that it represents a limiting case against which to assess and extend the validity of approaches developed to deal with spin-crossover systems. $[Fe(bpy)_3]^{2+}$ was thus studied with regard to the mechanism of the HS $\rightarrow$ LS relaxation after the photoinduced population of the HS state [24-29]. Recently, the mechanism of the photoinduced population of the HS state following excitation into the spin-allowed metal-ligand charge transfer (^{1}MLCT) band and the accompanying structural changes have also been studied for $[Fe(bpy)_3]^{2+}$ in solution by ultrafast UV-Vis and X-ray absorption spectroscopies [30-35].

The present review is organised as follows. We first deal with the DFT study of isolated complexes (Section 2) and then with their study in condensed phases (Section 3). Finally (Section 4), we conclude by putting the emphasis on the delicate issue of the accurate prediction of transition-metal spin-state energetics.

2. DESCRIPTION OF ISOLATED COMPLEXES: THE CASE STUDY OF $[Fe(bpy)_3]^{2+}$ IN THE FRAMEWORK OF HIGH-SPIN $\rightarrow$ LOW-SPIN INTERSYSTEM CROSSING

In spin-crossover complexes, the HS state can be populated as metastable state by photoexcitation. At cryogenic temperatures, the HS $\rightarrow$ LS relaxation proceeds through tunnelling and the relaxation rate can be so low that the complexes remain trapped in the HS state for up to several days. This is the phenomenon of light-induced excited spin state trapping (LIESST) [2, 36]. For first-row transition metal complexes, the HS $\rightarrow$ LS intersystem crossing is a radiationless non-adiabatic multiphonon process between two distinct zero-order spin states characterised by different geometries [37]. Since the metal-ligand bond experiences the largest structural changes upon the change of spin state, the totally symmetric breathing mode is naturally taken as the reaction coordinate Q, which, for the hexacoordinated complexes of interest reads: $Q = \sqrt{6}r$, where r is the average metal-ligand bond length. In this framework, the HS $\rightarrow$ LS tunneling rate constant can be written [2, 38]:

$$k_{HL}(T \rightarrow 0) = \frac{2\pi}{\hbar^2 \omega} \left|\beta_{HL}\right|^2 \left|\left\langle \chi_n \mid \chi_0 \right\rangle\right|^2 \quad (5)$$

where $\beta_{HL} = \left\langle \Phi_{LS} \mid H_{SO} \mid \Phi_{HS} \right\rangle$ is the electronic-coupling matrix element, which, for the iron(II) complexes with variation of the total electronic spin S of $\Delta S = 2$, originates from second-order spin-orbit coupling and takes on a value of $\left|\beta_{HL}\right| \approx 150\ cm^{-1}$ [37]. $\left|\langle \chi_n \mid \chi_0 \rangle\right|^2$ is the Frank-Condon factor, that is, the squared overlap integral of the vibrational wavefunction of the lowest vibrational level of the HS state with the one of the n-th LS vibrational level which ensures energy conservation. It depends on the relative horizontal and vertical displacements of the HS and LS potential wells, as respectively measured by Δr_{HL} or equivalently $\Delta Q_{HL} = \sqrt{6}\Delta r_{HL}$ and by ΔE_{HL}° or equivalently the reduced energy gap $n = \Delta E_{HL}^{\circ} / \hbar\omega$ (Fig. **1**). Assuming harmonic potentials and approximating these with equal force constants κ and vibrational frequencies $\hbar\omega$, taken as the respective averages of the real LS and HS values, the Franck-Condon factor can be expressed as:

$$\left|\left\langle \chi_n \mid \chi_0 \right\rangle\right|^2 = \frac{S^n e^{-S}}{n!}$$

where the Huang-Rhys factor:

$$S = \frac{1}{2} \frac{\kappa \left(\Delta Q_{HL}\right)^2}{\hbar\omega}$$

is a dimensionless measure of the relative horizontal displacement of the potential wells.

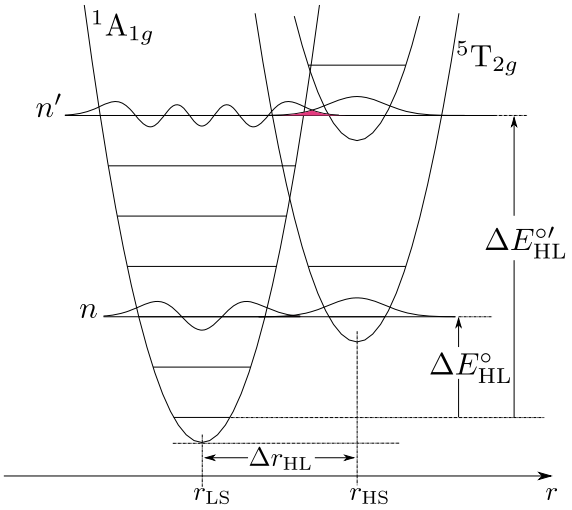

Fig. (1). Configurational diagram along the metal-ligand distance coordinate for octahedral Fe(II) complexes with a LS ground state. The potential curves of the LS $^1A_{1g}$ and HS $^5T_{2g}$ states are plotted assuming equal vibrational frequencies, $\hbar\omega$, for the two states. The shaded (red) areas represent the overlaps of the vibrational wavefunction of the lowest vibrational level of the HS state with the one of the LS vibrational level which ensures energy conservation for different values of the zero-point energy difference: $n = \Delta E^{\circ}_{HL} / \hbar\omega$, $n' = \Delta E^{\circ\prime}_{HL} / \hbar\omega$ and $\left|\langle\chi_n \mid \chi_0\rangle\right| < \left|\langle\chi_{n'} \mid \chi_0\rangle\right|$.

For the iron(II) spin-crossover complexes with a $[FeN_6]$ core, Δr_{HL} is in the range 0.16-0.22 Å. Consequently, using the model values of $\hbar\omega = 250$ cm^{-1} and $\kappa = 2\times10^5$ dyn cm^{-1}, S is estimated in the range 40-50 [2, 38]. Furthermore, estimates of ΔE°_{HL} in spin-crossover complexes are obtained from their $T_{1/2}$ values Eq. (4). In Fig. **2**, the low-temperature tunnelling rate constant is plotted as a function of ΔE°_{HL} for a series of iron(II) spin crossover complexes with a $[FeN_6]$ first coordination sphere: the full line is calculated according to Eq. (5) with $S = 45$, the broken lines with $S = 40$ and 50, respectively. The experimental points fall within the predicted interval, and the single-coordinate kinetic model thus quantitatively applies to the description of the low-temperature kinetics of the HS $\rightarrow$ LS relaxation in such complexes.

In LS complexes, the HS state can also be populated by photo-excitation. The study of the HS $\rightarrow$ LS relaxation dynamics proves to be a means for the indirect characterisation of the HS state. Proceeding along this line, we have extrapolated the single-coordinate kinetic model to the D_3 LS complex $[Fe(bpy)_3]^{2+}$ [39], which has the same $[FeN_6]$ first coordination sphere as the aforementioned iron(II) spin-crossover complexes. For $[Fe(bpy)_3]^{2+}$ doped into different inert crystalline host lattices, $k_{HL}(T \rightarrow 0)$ is found to range from *ca.* 10^4 s^{-1} to 10^8 s^{-1} [2]. Making use of the single-mode kinetic model with a model value of $S = 45$ for the Huang-Rhys factor, ΔE°_{HL} is predicted to vary between 2500 cm^{-1} and 5000 cm^{-1}, depending on the environment of the complex (Fig. **2**). This is consistent with the fact that the complex is a LS species.

Given that no experimental structural information on the geometry of the complex in the HS state was available at the time of the study, the essential assumption made in this approach is that, for $[Fe(bpy)_3]^{2+}$, $\Delta r_{HL} \approx 0.2$ Å, as for the iron(II) spin-crossover complexes with the same $[FeN_6]$ core. DFT applies to the lowest-lying state of each spatial and spin symmetry [40]. Hence, in order to test the structural assumption, the geometry of the D_3 $[Fe(bpy)_3]^{2+}$ complex in the LS $^1A_1$ state and in the ^5E and $^5A_1$ trigonal components of the HS state was optimized within DFT (upon $O_h \rightarrow D_3$ symmetry lowering, $A_{1g} \rightarrow A_1$ and $T_{2g} \rightarrow A_1 \oplus E$). Before going further in the presentation of the study, it is worth stressing that, due to the presence of partially filled d subshells, the description of transition metal complexes within the single-determinantal KS formulation of DFT is not self-evident.

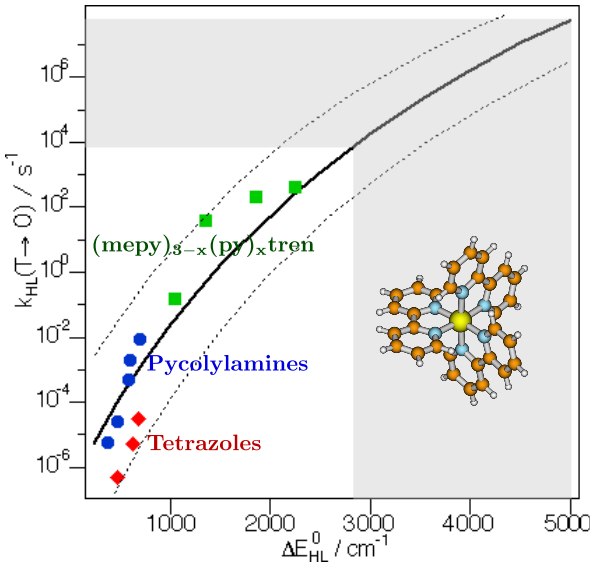

Fig. (2). Low-temperature tunnelling rate constant as a function of ΔE°_{HL}: the curves were calculated using for the Huang-Rhys factor (see Text) an average value of 45 , and limiting values of 40 and 50 (dashed lines). The symbols represent the experimental values for a series of spin-crossover compounds with a $[FeN_6]$ core [2]; and the shaded area, the range of experimental values found for the LS complex $[Fe(bpy)_3]^{2+}$ doped into different crystalline host lattices. Adapted from Ref [2, 39].

There are indeed fundamental issues in the application of the standard KS formalism to the study of open-shell systems [41-44]. In the following, we give a brief overview of these issues and of DFT approaches, which have been developed to address them in an approximate or in an exact manner. This overview is not meant to be exhaustive but to help delineate the framework within which DFT is routinely applied to the study of the transition metal complexes. Detailed and critical discussions about the implications of these issues and about the formal or pratical merits of the mentioned methods can be found in the referenced articles, which may serve the interested reader as a starting point to delve into the literature on the difficulties arising from the application of DFT to open-shell systems.

In the treatment of open-shell systems within the standard spin-unrestricted single-determinantal KS-DFT formalism, the charge and spin densities generally have a lower symmetry than the interacting electronic Hamiltonian,

which is invariant under the spatial symmetric group of the systems and which, assuming a nonrelativistic framework, commutes with the total electronic spin operator and is thus invariant with respect to rotations in spin space [41, 45, 46]. The symmetry of the KS Hamiltonian being given in a spin-restricted approach by the symmetry of the charge density and in a spin-unrestricted approach by the symmetry of the spin density, the KS Hamiltonians of open-shell systems do not generally have the full spin and spatial symmetry of the system and the KS wavefunctions consequently cannot be labelled according to the full symmetry group of the systems [41, 46]. The wavefunction of a multiplet state of a given spin and spatial symmetry generally cannot be given by a single determinant, even in the noninteracting case, but by a configuration state function, that is, by a symmetry-adapted linear combination of several determinants originating from the considered configuration [41, 46-48]. Furthermore, regarding the generalization of the KS scheme to the lowest-lying state of each spin and space symmetry, the conventional approximate functionals do not present the required dependence on the spin and spatial symmetries [40, 41, 46].

In practice, approximate approaches have been devised to bypass these difficulties and help achieve a description of open-shell systems from the results of standard KS-DFT calculations. These include, for instance, the multiplet sum method (MSM) of Daul [49], which is based on earlier developments by Ziegler, Rauk and Baerends [50], and the broken-symmetry (BS) approach of Noodleman [51, 52]. The MSM has been applied to the determination of multiplet splittings in transition metal complexes [49, 53-55], and the BS approach is used to study the magnetic coupling in transition metal clusters and extended systems [51, 52, 54, 56-64]. The latter also finds applications in the description of open-shell singlet biradicals [65, 66]. Recently, extensions of the KS formalism have been developed to cope within a spin-restricted DFT framework with the situations of strong static correlation, which are met with open-shell systems and are due to near or exact degeneracies. Thus, the "spin-restricted ensemble-referenced Kohn-Sham" (REKS) method of Filatov and Shaik [67, 68], enables one to tackle the electronic-structure problem within the desired spin and spatial symmetry, using conventional approximate functionals. In this extension of the KS formalism, the charge density of the state is given by a symmetry-adapted weighted sum of single-determinantal densities, while its energy is given by a corresponding weighted sum of single-determinantal energies. The REKS method has been applied to the study of bond-breaking processes and to the determination of singlet-triplet energy differences in biradicals and in Cu(II) binuclear complexes [65, 68-71]. We close this short survey with the symmetrized KS formalism of Görling, which allows for a proper treatment of open-shell states and especially of the lowest-lying state of each spin and spatial symmetry [41, 45, 46, 72]. In this formalism, the basic quantity is no longer the charge or the spin density but the totally symmetric contribution of the charge density of the lowest-lying state of a given irreducible representation of the point group symmetry of the considered system; the KS Hamiltonian is non-spin-polarized and totally symmetric in ordinary space; the KS wavefunctions are configuration state functions belonging to the same irreducible representations as the wavefunctions of the system; and the exchange and correlation energies are state-dependent functionals. However, while exchange can be treated exactly, accurate approximate state-dependent correlation functionals remain to be built [45, 46, 48, 72].

Interestingly however, despite the issues briefly outlined above, conventional KS-DFT methods often allow for an accurate description of open-shell systems such as transition metal complexes [43, 64]. That is, the single-determinantal framework of the standard KS formalism is often well-suited for studying these systems and the accuracy achieved is determined by the performance of the approximate exchange-correlation functional used [43]. This is the case when dealing with spatially non-degenerate multiplets. For characterizing one such state of total electronic spin S, the KS-DFT calculations are run restricted (closed shell, $S = 0$) or unrestricted ($S > 0$) while constraining M_S, the projection of the total electronic spin along a reference axis, to $M_S = S$. Within the given spin multiplicity, the lowest-lying state belonging to a given non-degenerate irreducible representation can be characterized by searching for the energetically lowest solution of the KS equations which belongs to the considered irreducible representation. Spatially degenerate multiplets are handled in the framework of ensemble KS DFT [13, 73]. Specifically, for a system in a g-fold spatially degenerate multiplet of total electronic spin S, the ↑- and ↓-spin densities are given by the respective arithmetic averages of the ↑- and ↓-spin densities of the g degenerate KS determinants, which span the degenerate irreducible representation and are obtained from unrestricted calculations carried out with $M_S = S$. The spin densities have the full spatial symmetry of the system. The occupation numbers f_i^σ of the KS σ -spin-orbitals are given by:

$$f_i^\sigma = \frac{1}{g}\sum_{k=i}^{g} \theta_{ki}^\sigma$$

where θ_{ki}^σ is the occupation of the i- th σ-spin-orbital in the k-th KS determinant ($\sigma = \uparrow, \downarrow$). The occupation numbers are fractional for the partially occupied degenerate spin-orbitals. This is the reason why the characterization of spatially degenerate multiplets requires the use of quantum chemistry codes which allow fractional occupation numbers.

For characterizing $[Fe(bpy)_3]^{2+}$ in the LS $^1A_1$ state and in the HS ^5E and $^5A_1$ states, the geometry optimizations was performed with the BP86 [74-76], PW91 [77-80], PBE [81, 82] and RPBE [83] GGAs and the B3LYP [84], B3LYP* [85-87] and PBE0 [88, 89] global hybrids. The results showed that the metal-ligand bond experiences the largest structural change upon the change of spin-states. Furthermore, the predicted values of Δr_{HL} are close to the assumed value of 0.2 Å (Fig. **3**), thus validating the extension of the single-coordinate kinetic model to the LS complex $[Fe(bpy)_3]^{2+}$ [39].

$[Fe(bpy)_3]^{2+}$ and $[Fe(tpy)_2]^{2+}$ (tpy = 2,2':6',2''-terpyridine) are two chemically very similar polypyridinyl complexes. They both are LS species up to well above room temperature and, after the photoinduced LS → HS transition, they both show comparatively fast HS → LS intersystem crossing with $k_{HL}(T \to 0) \geq 10^4$ s^{-1}. However, $[Fe(tpy)_2]^{2+}$ can be trapped

at low temperatures in the HS state when doped into specific crystalline hosts [29, 90, 91]. In these cases, the use of the single-mode kinetic model would lead to the wrong conclusion that $[Fe(tpy)_2]^{2+}$ is a spin-crossover complex. Indeed, DFT calculations performed on $[Fe(tpy)_2]^{2+}$ in the two spin states confirmed that the single-coordinate model does break down for this complex [29]. While the Fe-N bonds still substantially lengthen upon the LS $\rightarrow$ HS change of states, the $[FeN_6]$ first coordination sphere in $[Fe(tpy)_2]^{2+}$ actually undergoes a strongly anisotropic distortion, whose description requires the inclusion of at least one mode in addition to the breathing mode. The additional modes, corresponding to twisting motions from D_{2d} towards D_2 symmetry, are responsible for the large increase of the barrier and the concomittant decrease of the relaxation rate. The fact that the trapping of the HS state in $[Fe(tpy)_2]^{2+}$ is observed for the complex in some environments and not in others could be ascribed to the fact that the latter environments cannot accomodate the distortion of the complex [29]. The success met with the application of DFT to the analysis of the HS $\rightarrow$ LS intersystem crossing in these LS iron(II) species follows from the ability of most functionals beyond the local density approximation (LDA) [19, 92-97] to correctly describe the geometries of transition metal complexes in the LS and HS states [98].

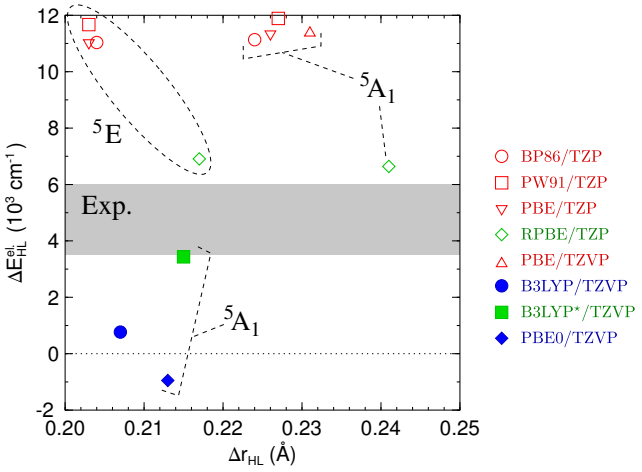

Fig. (3). Plot of the calculated HS-LS electronic energy differences ΔE^{el}_{HL} against the predicted values of the HS-LS bond length change Δr_{HL} for $[Fe(bpy)_3]^{2+}$ [39]. All functionals predict $\Delta r_{HL} \approx 0.2$ Å. The experimental estimate of ΔE^{el}_{HL} (shaded area) is overestimated by most GGAs (red symbols), underestimated by the standard global hybrids including 20~25% of exact exchange (blue symbols), and approached by the GGA RPBE and the global hybrid B3LYP* (green symbols). The calculations were carried out using Slater-type (TZP) and Gaussian-type (TZVP) basis sets of triple-ζ polarized quality, which perform similarly as attested for by the PBE/TZP and PBE/TZVP results. See Ref. [39] for the computational details.

The HS-LS zero-point energy difference can be divided into a vibrational, ΔE^{vib}_{HL}, and an electronic contribution, ΔE^{el}_{HL}:

$$\Delta E^{\circ}_{HL} = \Delta E^{el}_{HL} + \Delta E^{vib}_{HL} \quad .$$

DFT methods tend to perform reasonably well for the calculation of the vibrational frequencies of transition metal complexes. The calculations are performed within the harmonic approximation. As discussed by Paulsen and Trautwein [98], the results are used for in-depth analyses of the infrared, Raman and inelastic neutron scattering spectra of the complexes, and also for the evaluation of their HS-LS vibrational energy and entropy differences. However, due to the neglect of the environmental effects in the calculations performed in the gas phase, significant discrepancies can be observed between calculated and experimental vibrational properties. [86, 98, 99] In the study of $[Fe(bpy)_3]^{2+}$ in the framework of the HS $\rightarrow$ LS relaxation [39], the gas-phase vibrational analysis led to a ΔE^{vib}_{HL} estimate of -875 cm^{-1}, from which the best experimental estimate of ΔE^{el}_{HL} for $[Fe(bpy)_3]^{2+}$ was determined to be in the 3500-6000 cm^{-1} range. But the ΔE^{el}_{HL} values calculated with the GGA and global hybrid functionals vary between -1000 and 16000 cm^{-1}. That is, depending on the functional, $[Fe(bpy)_3]^{2+}$ is predicted to be a HS, a spin-crossover or a LS species.

Fig. **3** gives for $[Fe(bpy)_3]^{2+}$ the plot of the calculated ΔE^{el}_{HL} values against the predicted values of Δr_{HL}, while allowing the comparison of experiment and theory for the spin-state energetics. Its inspection shows that the Fe-N bond is only around 0.02 Å longer in the $^5A_1$ state than in the ^5E state. The similar geometries of the $^5A_1$ and ^5E states as well as their near-degeneracy as consistently predicted by the functionals (Fig. **3**) follow from the fact that passing from one high-spin state state to the other mainly involves an electronic rearrangement in nonbonding metallic levels of octahedral t_{2g} parentage. One also notes in Fig. **3** that the Δr_{HL} values obtained with the PBE0, B3LYP and B3LYP* global hybrids are slightly smaller than those obtained with the GGAs. Actually, the hybrid functionals tend to give longer metal-ligand bonds than their GGA analogues and these bonds will be longer the larger the exact-exchange contribution. The smaller Δr_{HL} values obtained with the hybrids follow then from the fact that the increase of the metal-ligand distance with the amount of exact exchange is faster in the LS than in the HS state (see Fig. **8** in Ref. [39]). Given that correlation is more important in the LS state than in the HS state, the subtle dependence of the optimized metal-ligand bond lengths on the exact-exchange contribution in global hybrids reflects the enhancement of exchange and the concomitant turning off of correlation with increasing amount of exact exchange [100].

Spin crossover and related phenomena occur in condensed phases. However, as illustrated by the DFT study of $[Fe(bpy)_3]^{2+}$ in the framework of the HS $\rightarrow$ LS relaxation, their computational study generally involves calculations performed on the isolated complexes in the gas phase, while the perfomances of the computational methods are assessed by comparing their gas-phase results against the experimental data. The underlying assumption is that the environment of the complexes has a weak influence on the investigated properties. For $[Fe(bpy)_3]^{2+}$, this assumption holds for the determination of the HS-LS bond length difference Δr_{HL} (see below). It however breaks down for the evaluation of the HS-LS energy difference, which indeed varies by as much as 2500 cm^{-1} for $[Fe(bpy)_3]^{2+}$ doped into different crystalline hosts (Fig. **3**). Nevertheless, in the

absence of accurate relevant gas-phase references, the ability of the computational methods to give results close to the experimental estimates of the HS-LS energy differences remains our main criterion for assessing their performance.

As dicussed in detail in Ref. [39], the difficulties met with the exchange-correlation functionals for the accurate determination of transition-metal spin-state energetics can be ascribed to their inability to correctly account for the variation of the exchange interaction with increasing or decreasing spin polarisation and also with significant differences in bond lengths [100, 101]. That the exchange functional is to be blamed is illustrated (*i*) by the very different results obtained with the PBE, RPBE and PBE0 functionals, which share the same correlation functional, and (*ii*) by those obtained with the B3LYP and B3LYP* hybrid functionals, which only differ by their exact-exchange contributions (Fig. **3**). The GGAs inherit the underestimation of exchange from their LDA components. Among the GGAs used, the largest gradient corrections of the RPBE exchange [83] thus explain the improved results obtained with the RPBE exchange-correlation functional. Exchange is overestimated by the PBE0 and B3LYP hybrids incorporating some 20% of exact exchange. With its 15% of exact-exchange contribution, the B3LYP* functional of Reiher and coworkers [85-87], tailored to the spin-state energetics of other iron(II) complexes, performs better. The study of the dependence of ΔE_{HL}^{el} on the exact-exchange contribution indicated that this one should effectly be reduced to some 10% in both the PBE0 and B3LYP hybrids to achieve an improved description of the spin-state energetics of $[Fe(bpy)_3]^{2+}$ [39].

The detailed study of $[Fe(bpy)_3]^{2+}$ did not allow us to discriminate between correlation functionals with different formal properties. The rearrangement of the electronic structure upon the change of spin states mostly take place in the compact *3d* shell. Therefore, the fact that exchange dominates the high-density limit [81, 82] probably explains why the limitations of the exchange functionals prove to be those exacerbated by the issue of the accurate evaluation of transition-metal spin-state energetics. The transition-metal spin-state energetics issue in DFT has been tackled by different research groups [22, 23, 55, 85-87, 98, 102-127]. However, no exchange-correlation functional has emerged so far as the functional of choice for addressing this issue, which actually also shows up with wavefunction-based methods (see Section **4**).

3. CONDENSED-PHASE STUDIES: PROBING THE ROLE OF THE ENVIRONMENT

Achieving an in-depth understanding of spin crossover and related phenomena requires that the environment of the complexes be taken into account as accurately as possible in order to be able to get insight into the nature of the interactions between the complexes and their environment and into how the latter evolves with the change of spin states. This is discussed in the following using as examples two of our studies, which deal with the description of $[Fe(bpy)_3]^{2+}$ in aqueous solution and encapsulated in the supercage of zeolite Y.

3.1. Spin-State Dependence of the Dynamic and Microscopic Structure of Aqueous $[Fe(bpy)_3]^{2+}$

The mechanism of the HS $\rightarrow$ LS relaxation is well understood in terms of a non adiabatic multiphonon process [2]. In contrast, the mechanism of the photoinduced LS $\rightarrow$ HS transition remains a vivid subject of current research. It was thus recently studied in Fe(II) spin-crossover complexes [128-134] and in the LS complex $[Fe(bpy)_3]^{2+}$ in solution [30-34, 135] using ultrafast time-resolved optical, vibrational and X-ray absorption spectroscopies. The emerging consensus is summarized in Fig. **4**.

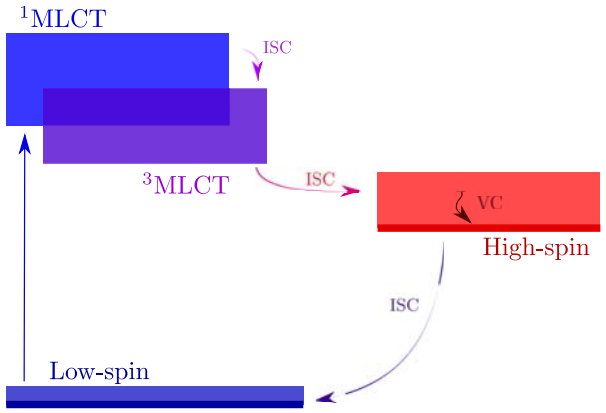

Fig. (4). Scheme of the currently accepted mechanism of the photoinduced spin crossover in iron(II) complexes in solution on irradiation into the ^{1}MLCT transition (MLCT: metal-to-ligand charge transfer; ISC: intersystem crossing; VC vibrational cooling).

Thus, upon photoexcitation into the singlet metal-to-ligand charge transfer (^{1}MLCT) manifold, there is a first intersystem crossing into the ^{3}MLCT manifold followed by a second one taking the molecule to a hot HS state. The hot HS state is formed on a subpicosecond timescale (~100 fs) and the vibrational cooling in the HS state occurs on a timescale of a few to one or several tens of picoseconds depending on the complex, the temperature and the solvent. While these studies accurately inform on the reaction coordinate of the Fe(II) chromophore upon photoexcitation, they leave open the questions regarding the structural changes undergone by the ligands, the influence of the solvent on the early evolution of the complex, the involvement of the solvent in the dissipation of the excess energy, and the response of the solvation shell to the perturbation. Answerning these questions is challenging from both theoretical and experimental points of view.

We have recently characterized the structure at room temperature of $[Fe(bpy)_3]^{2+}$ in aqueous solution and the organization of its solvation shell in the LS and HS states [136]. The study consisted in Car-Parrinello molecular dynamics (CPMD) simulations [137, 138] performed at 300 K with the BLYP functional [74, 139] using a 21 Å cubic simulation box containing $[Fe(bpy)_3]^{2+}$, two Cl^- counterions and 298 water molecules. The durations of the recorded LS and HS trajectories are about 24.5 ps and 4.0 ps, respectively. The shorter duration of the HS trajectory reflect the increase in the computational cost tied to the fact that the calculations are run restricted in the LS state and unrestricted

in the HS state. Fig. **5** shows a snapshot of the HS trajectory displaying water molecules and their hydrogen bond network, a counterion, $[Fe(bpy)_3]^{2+}$, and the spin density, which is centered on the iron atom and whose shape shows that, as expected, spin polarization occurs in the frontier metallic $3d$ orbitals of octahedral t_{2g} and e_g parentage.

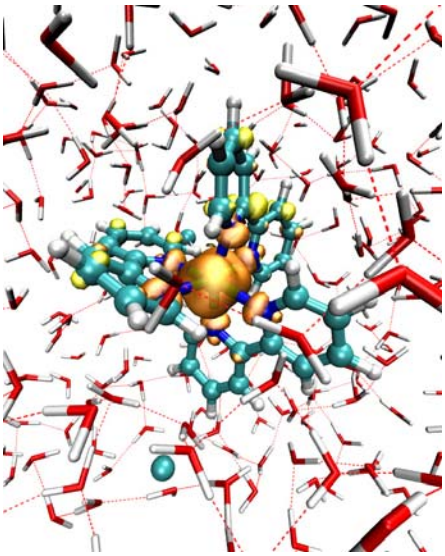

Fig. (5). Molecular dynamics study of $[Fe(bpy)_3](Cl)_2$ in water [136]: snapshot from the HS trajectory. Reprinted with permission from Ref. [136]. Copyright 2010 American Chemical Society.

The LS $\rightarrow$ HS crossover involves the promotion of two electrons from those metallic nonbonding levels of t_{2g} parentage into those antibonding of e_g parentage. The analysis of the trajectories showed that the resulting weakening of the metal-ligand bonds gives rise to a lengthening of the Fe-N bonds of $\Delta r_{HL} \approx 0.2$ Å, in agreement with our gas-phase calculations as well as the experimental results obtained by Chergui and coworkers using ultrafast X-ray absorption spectroscopy [30, 33]. Fig. **6** shows the thermal distributions of the Fe-N distances in the LS and the HS states. One notes that, besides the lengthening of the metal-ligand bond, its weakening also translates into a broadening of the distribution. The fits of the distributions with Gaussian distribution functions (Fig. **6**) gave average LS and HS Fe-N distances of $r_{LS} = 1.982 \pm 0.056$ Å and $r_{HS} = 2.173 \pm 0.079$ Å, respectively. The HS distribution actually presents a long tail, which was ascribed to the increased anharmonicity of the Fe-N bond in the HS states.

The weakening of the Fe-N bond proved to be also responsible for the increased thermal fluctuation of the whole molecular edifice. Further insight into the spin-state dependence of the room-temperature aqueous structure of $[Fe(bpy)_3]^{2+}$ could be gained from the comparison of the LS and HS aqueous structures with that of the LS d^6 $[Ru(bpy)_3]^{2+}$ complex, as determined by Röthlisberger and coworkers from a combined quantum mechanics/molecular mechanics (QM/MM) and classical molecular dynamics study [140]. Indeed, the Ru-N bond length of 2.077 Å is intermediate between the LS and HS bond lengths, and the arrangements of the bpy ligands about the metallic center are intermediates between those found in the LS and HS solution structures of $[Fe(bpy)_3]^{2+}$. Furthermore the thermal fluctuations are smaller in the ruthenium complex, wherein the metal-ligand bond is stronger than in $[Fe(bpy)_3]^{2+}$. It could be concluded that the arrangement of the bpy ligands in a $[M(bpy)_3]^{2+}$ complex is determined by the M-N equilibrium distance, while their thermal fluctuations are dictated by the strength of the M-N bond.

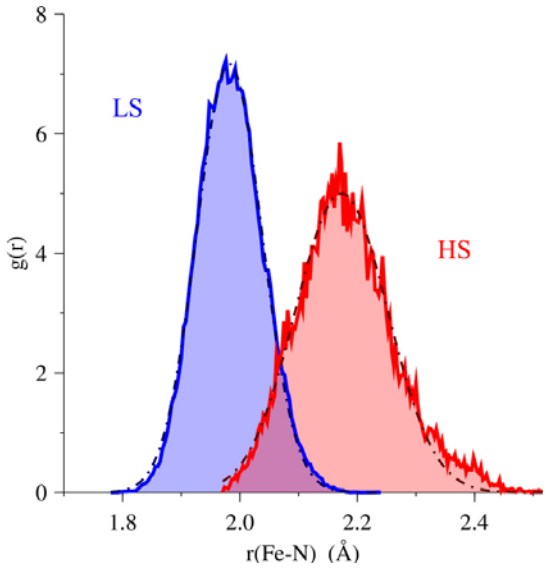

Fig. (6). Molecular dynamics study of $[Fe(bpy)_3](Cl)_2$ in water: thermal distributions of the Fe-N bond length in the LS and HS states (solid lines) and fits of the data assuming a Gaussian distributions (dashed lines). Adapted from Ref. [136].

The LS and HS radial distribution functions (RDFs) of the water oxygen atoms with respect to the iron atom are shown in Fig. **7**, along with the running coordination numbers. They help describe the organization of the solvent around $[Fe(bpy)_3]^{2+}$ in the two spin states. The two RDFs are very similar. They show a first broad peak with a maximum at ~5.7 Å and a minimum at ~6.3 Å, which defines the first solvation shell, and a second one centered at ~7.6 Å, which defines the second solvation shell. These RDFs are similar to the one determined for aqueous $[Ru(bpy)_3]^{2+}$ [140]. That is, the short-range order of water near a $[M(bpy)_3]^{2+}$ complex tends to be preserved upon transmetallation or a change of spin states. In particular, the first solvation shell consists of chains of water molecules intercalated between the ligands (see the inset of Fig. **7**). For $[Fe(bpy)_3]^{2+}$, the number of water molecules in the first solvation sphere was predicted to decrease from ~17 to ~15 on going from the LS to the HS state, which is supported by the results of a recent time-resolved X-ray spectroscopy study of aqueous $[Fe(bpy)_3]^{2+}$ [135] .

The nature of the solvent can significantly affect the thermal spin transition and the kinetics of the HS $\rightarrow$ LS relaxation which follow the photo-induced population of the HS state. This strengthens the need to explicitely take into account the organization of the solvent molecules around the complexes for the study of these phenomena in solution. Therefore, in order to achieve an in-depth understanding of the spin-state dependence of the dynamic and microscopic

structures of LS and spin-crossover iron(II) complexes in solution while getting a broad view of the involved solute-solvent interactions, we are extending the *ab initio* molecular dynamics study of aqueous $[Fe(bpy)_3]^{2+}$ to various LS and spin-crossover iron(II) complexes in different solvents. The simulation durations are to be increased so as to have better statistics in the two spin states. In particular, we expect to learn a lot from the comparative study of the LS complexes $[Fe(bpy)_3]^{2+}$ and $[Fe(tpy)_2]^{2+}$ in water and in acetonitrile. The bidentate bpy and trisdentate tpy ligands are indeed chemically very close but their trigonal and tetragonal coordination motives may translate into drastic differences between the solvation shells of the two complexes, in addition to those between their HS → LS relaxation coordinates, with important consequences for their photophysical properties.

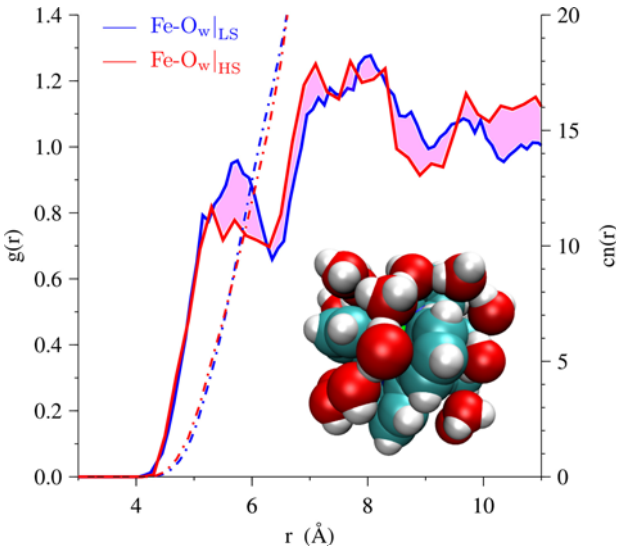

Fig. (7). Molecular dynamics study of $[Fe(bpy)_3](Cl)_2$ in water: LS and HS radial distribution functions $g(r)$ of the water oxygen atoms (O_w) with respect to the Fe atom (solid lines, left y-axis) and running coordination numbers $cn(r)$ (dashed lines, right y-axis). Inset: snapshot from the LS trajectory showing the first solvation shell of the complex. Adapted from Ref. [136].

3.2. Supramolecular Approach to the Study of the Influence of the Second Coordination Sphere in Inclusion Compounds

The molecular volume of $[Fe(bpy)_3]^{2+}$ being ≈20 Å^3 larger in the HS state than in the LS state, Hauser and coworkers [28] have shown that the manner in which the environment influences the spin-state energetics of the complex can be understood in terms of an internal or chemical pressure effect which destabilizes the HS state with respect to the LS state. More generally, the concept of chemical pressure was shown to provide insight into how the relative energies of the ligand-field states of the complexes $[M(bpy)_3]^{2+}$ (M = Fe, Ru, Co) and consequently their electronic properties can be tuned by guest-host interactions [28]. Of longstanding and widespread use in condensed-matter physics and chemistry (see, for instance, Refs. [141-145], this concept helps establish a parallel between the effect of the external pressure on a property of a material and the effect on this same property of a lattice volume variation obtained by chemical changes. Still, chemical pressure is not necessarily equivalent to the external pressure [146, 147]. Most importantly, the concept of chemical pressure unfortunately does not provide a detailed picture of the involved interactions.

Inclusion compounds are very attractive materials for an in-depth characterization of the guest-host interactions at the origin of the influence of the second coordination sphere on the properties of transition metal complexes. They indeed provide well-defined, stable and rigid frameworks, with cavities of various sizes and shapes, so that the encapsulation of transition metal complexes in these cavities allows for controlled variation of their second coordination environment. This is the case for zeolites with encapsulated transition metal complexes [148-153]. In particular, the supercage of zeolite Y, with a diameter of about 13 Å and openings of approximatively 7.4 Å [154], allows the encapsulation of organometallic molecules of a similar size, such as tris(2,2-trisbipyridine) complexes, using a ship-in-a-bottle synthesis [155-157]. The physicochemical properties of the zeolite-Y embedded $[Fe(bpy)_3]^{2+}$ complex ($[Fe(bpy)_3]^{2+}$@Y) have been the subject of several studies [157-161]. On the basis of their results, the supramolecular model of Fig. **8** was devised to get a detailed picture of the guest-host interactions in $[Fe(bpy)_3]^{2+}$@Y and to get insight into their influence on the structural, Mössbauer spectroscopy and energetic properties of the complex [162].

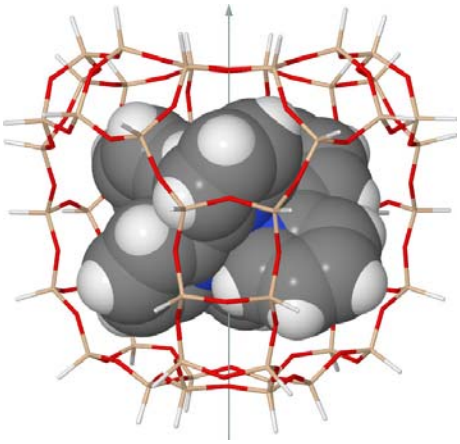

Fig. (8). Supramolecular model used for the description of the inclusion compound $[Fe(bpy)_3]^{2+}$@Y [162].

The model consists of the complex $[Fe(bpy)_3]^{2+}$ and the neighboring Si and O atoms which define the supercage, and the valence of the Si atoms being saturated with H atoms. The relative orientation of the two subsystems is such that the model is of C_3 symmetry, with the trigonal axis of the complex coinciding with one C_3 axis of the supercage, which has an ideal T_d symmetry. The LS and HS geometries of the model and also those of the free complex were optimized within DFT using the PBE, HCTH [163] and OLYP [139, 164] GGAs and the B3LYP* and O3LYP [164] hybrid functionals. In either spin state, the different functionals gave geometries which are very similar, like for the free complex. The optimal orientation found for the complex in the supercage helps minimize the steric repulsion between the two

subsystems, with the C-H bonds of each bipyridine facing a twelve- or a six-membered opening and pointing into the void (Fig. **8**). Upon encapsulation, the complex slightly contracts and distorts for a best fit into the supercage. As shown in Fig. **9**, the distortion is more pronounced in the HS state than in the LS state, because of the larger molecular volume of $[Fe(bpy)_3]^{2+}$ in the HS state.

For the encaged complex, the major structural change experienced upon the LS $\rightarrow$ HS change of states is the lengthening of the metal-ligand bond of $\Delta r_{HL} \approx 0.2$ Å, as for free or aqueous $[Fe(bpy)_3]^{2+}$. Because of the rigidity of the host, the structural changes undergone by the supercage upon the inclusion of the LS complex are minimal and the large expansion of the guest complex in passing from the LS to the HS state hardly affects its geometry [162].

^{57}Fe Mössbauer spectroscopy [165, 166] is an efficient and widely-used tool for the quantitative study of spin crossover in iron compounds [7]. It indeed gives two parameters which are sensitive to the redox state, the spin state and the bonding environment of iron sites: namely, the isomer shift δ, which depends on the electronic charge density at the iron nucleus, and the quadrupole splitting ΔE_Q for the ^{57}Fe $I = 3/2$ excited nuclear state, which informs about the anisotropy of the electric field gradient at the Fe nucleus. Both parameters can be determined quite accurately within DFT [98, 167-172]. For the zeolite-Y encapsulated LS $[Fe(bpy)_3]^{2+}$ complex, the Mössbauer parameters accurately determined by Vankó and coworkers are $\delta = 0.32$ mm s^{-1} and $|\Delta E_Q| = 0.32$ mm s^{-1} [159]. Given that these parameter values are similar to those measured for $[Fe(bpy)_3]^{2+}$ in other environment and that ΔE_Q gives a measure of the distortion undergone by the complex upon encapsulation, these authors could conclude that the LS complex did not undergo major distortions upon encapsulation. The fact that the same conclusion could be drawn from the computational study of $[Fe(bpy)_3]^{2+}$@Y validates the supramolecular approach used.

ΔE_Q has been calculated for the isolated and the encaged complex in the LS ^{1}A and in the HS ^{5}A and ^{5}E states (see Ref. 162 for the computational details). For the isolated LS $[Fe(bpy)_3]^{2+}$, $\Delta E_Q \approx -0.39$ mm s^{-1}. Upon encapsulation, the magnitude of ΔE_Q decreases, ΔE_Q taking values between -0.38 and -0.32 mm s^{-1} depending on the functional used for the geometry optimization. There is for $|\Delta E_Q|$ a good agreement between experiment and theory. The best agreement being observed for the geometries obtained with HCTH, O3LYP and OLYP functionals, it could be concluded that these functionals perform better for the description of the structure of the encapsulated complex. For the free complex in the HS ^{5}E state, the calculations gave $\Delta E_Q \approx +1.33$ mm s^{-1} and, upon encapsulation, ΔE_Q is predicted to increase to about +1.37 or +1.40 mm s^{-1} depending on the functional used for the optimization. The calculations similarly performed for $[Fe(bpy)_3]^{2+}$ in the HS ^{5}A state gave $\Delta E_Q \approx -2.68$ mm s^{-1} in the gas phase. Although the value taken in the ^{5}A state upon encapsulation could not be determined, it is expected to be close to the gas-phase value of about -2.7 mm s^{-1}. From the Mössbauer emission spectroscopy study of $[^{57}Co/Mn(bpy)_3](PF_6)_2$, Deisenroth and coworkers have determined the Mössbauer parameters of $[Fe(bpy)_3]^{2+}$ in the HS state [25]. Thus, for the nucleogenic HS $[^{57}Fe(bpy)_3]^{2+}$ complex $|\Delta E_Q| \approx 1.17$ mm s^{-1}. From the good agreement between this value and those calculated for the complex in the ^{5}E state, it could be inferred that the ^{5}E state is the lowest-lying component of the HS state for $[Fe(bpy)_3]^{2+}$ doped into $[Mn(bpy)_3](PF_6)_2$. Given that the two trigonal components of the high-state are nearly degenerate for the isolated complex and that its molecular volume is slightly larger in the ^{5}A state than in the ^{5}E state [39], the fact that the ^{5}E state is the lowest-lying HS component in the $[Mn(bpy)_3](PF_6)_2$ crystalline host was acribed to the chemical pressure experienced by $[Fe(bpy)_3]^{2+}$, which destabilizes the ^{5}A state with respect to the ^{5}E state. The same energy ordering, is expected for the zeolite-Y embedded $[Fe(bpy)_3]^{2+}$ complex: $E(^5E) \leq E(^5A)$ [162]. The Mössbauer parameters of $[Fe(bpy)_3]^{2+}$@Y in the HS state cannot be determined experimentally because of the very short lifetime τ_{HS} of this state. However, from the time-integral Mössbauer emission spectroscopy intensity data of $[^{57}Co(bpy)_3]^{2+}$@Y, Vankó and coworkers could determine $\tau_{HS} < 60$ ns or equivalently $k_{HL}(T \rightarrow 0) > 1.7 \times 10^7$ s^{-1} [27]. Making use of the single-coordinate kinetic model of relaxation of Hauser (Fig. **2**), this gives for ΔE°_{HL} in $[Fe(bpy)_3]^{2+}$@Y a lower limit of *ca.* 5000 cm.

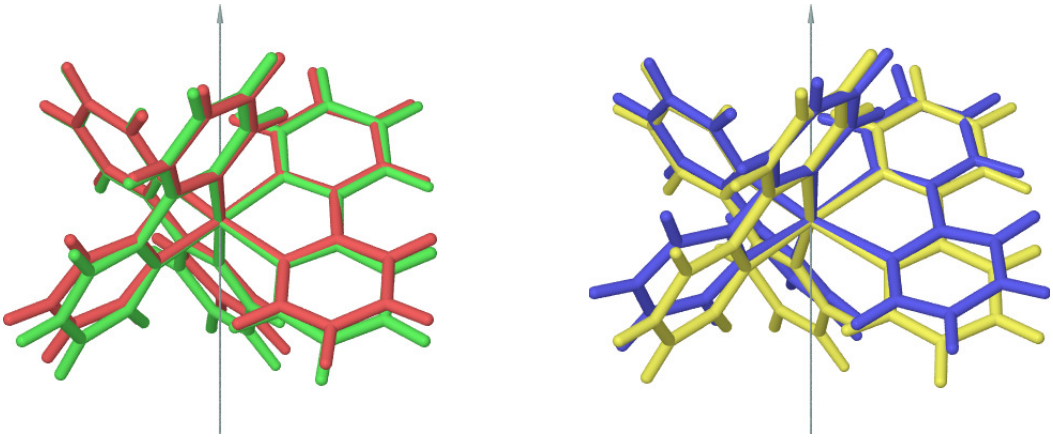

Fig. (9). Influence of encapsulation on the structure of $[Fe(bpy)_3]^{2+}$ (OLYP results) [162]: (left) superimposed LS geometries of $[Fe(bpy)_3]^{2+}$ in the gas phase (green) and in $[Fe(bpy)_3]^{2+}$@Y (red); (right) superimposed HS geometries of $[Fe(bpy)_3]^{2+}$ in the gas phase (yellow) and in $[Fe(bpy)_3]^{2+}$@Y (blue).

The calculated HS-LS electronic energy differences exhibit the usual strong dependence on the functional used, ranging from −811 to 10087 cm^{-1} for $\Delta E_{HL}^{el}[\varnothing]$, the value of ΔE_{HL}^{el} in $[Fe(bpy)_3]^{2+}$, and from 1941 to 12004 cm^{-1} for $\Delta E_{HL}^{el}[Y]$, the value of ΔE_{HL}^{el} in $[Fe(bpy)_3]^{2+}@Y$. Remarkably however, the different functionals gave very consistent values for the change $\Delta(\Delta E_{HL}^{el})$ in ΔE_{HL}^{el}: $\Delta(\Delta E_{HL}^{el}) = \Delta E_{HL}^{el}[Y] - \Delta E_{HL}^{el}[\varnothing]$. The $\Delta(\Delta E_{HL}^{el})$ values are positive and in the narrow range of 1917-2934 cm^{-1}. That is, the HS state is destabilized with regard to the LS state upon encapsulation and the functionals perform similarly well for quantifying the influence of the guest-host interactions in $[Fe(bpy)_3]^{2+}@Y$ on the HS-LS energy difference. A fair estimate of $\Delta(\Delta E_{HL}^{el}) = 2500 \pm 1000$ cm^{-1} was obtained [162]. Using the CASPT2 estimate of $\Delta E_{HL}^{el}[\varnothing]$ of 3700 ± 1000 cm^{-1} determined by Pierloot and Vancoilie [119, 173], this result led to $\Delta E_{HL}^{\circ}[Y] = 5400 \pm 1500$ cm^{-1}, which is close to the lower limit given above.

$\Delta(\Delta E_{HL}^{el})$ divides into two contributions: (1) a geometric distortion contribution $\Delta E_{HL}^{dist} = E_{HS}^{dist} - E_{LS}^{dist}$, where E_{Γ}^{dist} is the energy required to bring the separated guest and host from their relaxed geometries to their geometries in $[Fe(bpy)_3]^{2+}@Y$ in the Γ spin state; and (2) a contribution $\Delta E_{HL}^{int} = E_{HS}^{int} - E_{LS}^{int}$, which is the change in the guest-host interaction energy E^{int} upon the LS $\rightarrow$ HS change of state. $\Delta E_{HL}^{dist} > 0$, thus reflecting the fact that the distortions undergone by the subsystems are more pronounced in the HS state than in the LS spin state. Of the two contributions to $\Delta(\Delta E_{HL}^{el})$, ΔE_{HL}^{dist} turned out to be the one responsible for the dispersion observed in the predicted $\Delta(\Delta E_{HL}^{el})$ values, while $\Delta E_{HL}^{int} \approx +1300$ cm^{-1} for the different functionals used. The influence of the choice of the functionals on ΔE_{HL}^{dist} is discussed in details in Ref. [162]. Here we focus on the analysis reported therein for ΔE_{HL}^{int}.

Making use of the Morokuma-type energy decomposition scheme implemented in the ADF program package [174-178], E^{int} was decomposed into three contributions: (1) E^{elstat}, which is due to the electrostatic interaction between the unperturbed charge distributions of the subsystems at their geometries in $[Fe(bpy)_3]^{2+}@Y$, the total electron density being the simple superposition of their densities; (2) the Pauli repulsion term E^{Pauli}, which is reponsible for the steric repulsion between the subsystems and which is the energy change upon going from the superposition of the subsystem densities to the wavefunction that obeys the Pauli principle by the antisymmetrization and normalization of the product of the substystem wavefunctions; and finally, (3) the orbital interaction energy E^{orb}, which is the energy gained by relaxing the electron density.

In both spin states, the guest-host interactions are stabilizing: $E^{int} < 0$. The attractive contributions E^{elstat} and E^{orb} are smaller in magnitude than the Pauli repulsion E^{Pauli}, which they do more than compensate. With $E^{elstat} < E^{orb} < 0$, the bonding between $[Fe(bpy)_3]^{2+}$ and the cage is more electrostatic than covalent. Upon the LS $\rightarrow$ HS change of states, the expansion of $[Fe(bpy)_3]^{2+}$ translates into an increase of the Pauli repulsion, which was found to represents only ~53% of ΔE_{HL}^{int}. The electrostactic and orbital interactions also become less attractive and the associated energy changes correspond to ~25% and ~22% of ΔE_{HL}^{int}, respectively. At a given geometry of $[Fe(bpy)_3]^{2+}@Y$, the guest-host interactions were shown to not vary upon a change of spin states because of the strongly local character of the involved d –d transition, but also upon the substitution of Fe^{2+} with the $4d^6$ Ru^{2+} and $3d^{10}$ Zn^{2+} ions. The guest-host interactions in $[M(bpy)_3]^{2+}@Y$ could then be defined as the closed-sheel interactions between the first coordination sphere provided by the bpy ligands and the second coordination sphere defined the supercage, under the polarizing influence of the M^{2+} transition metal ion. The picture thus obtained for the guest-host interactions remains the same if one actually considers other valences for the transition metal ions.

To go further in the study of $[Fe(bpy)_3]^{2+}@Y$, the model of the zeolite-Y host can be refined by decorating the supercage with the neighoring sodalite cages, which may make the model more rigid, or by substituting Si(IV) with Al(III) in order to reproduce the negatively charged backbone of the host. The supramolecular approach used is of wide applicability. It can for instance be used to study how the oxidation catalytic activities of metalloporphyrins are influenced by their encapsulation in zeolites [152, 179-181] or in metal-organic frameworks [182, 183]. The underlying bonding energy decomposition scheme applies to the study of guest-host binding in self-assembled molecular coordination cages [184-187]. In particular and of interest to us, it would help understand how the encapsulation of square planar Ni(II) and Co(II) complexes into such cages induces the low-spin $\rightarrow$ high-spin spin crossover with no obvious changes in the coordination geometry or number, as reported by Yoshizawa, Fujita and coworkers [188]. In this case especially, and for guest-host assemblies in general, the analysis of the guest-host interactions would also benefit from the use of methods, such as the analysis of the electron density based on the quantum theory of atoms in molecules [189, 190] , the electron localization function [191-194], the electron localizability indicator [195-197], or the maximally localized Wannier functions [198], which allow to get an insightful picture of the nature of the intermolecular bonds in the liquid or in the solid state.

The periodic DFT study of the spin-crossover materials is necessary when molecular spin-crossover entities cannot be isolated, as in polymeric spin-crossover networks [199, 200]. It is also essential to the understanding of stacking and counterion effects [201-203], of temperature and pressure effects [204, 205], and of the manner in which the macroscopic properties of the materials are affected by changes, which, like spin crossover, occur at the molecular level.

4. CONCLUDING REMARKS: TOWARDS ACCURATE SPIN-STATE ENERGETICS

Using the study of the LS complex $[Fe(bpy)_3]^{2+}$ in the gas phase and in condensed phases as a guideline, we have tried to give an overview of the different aspects of the application of DFT to the study of transition metal complexes in the framework of spin crossover or related phenomena. Accurate results can be obtained for the structural, vibrational, and Mössbauer spectroscopy properties of the complexes in the LS and HS states, and also for their energetics within a given

spin multiplicity. The inclusion of environmental effects in the studies is key to the understanding of the phenomena, and this can as well be accurately achieved within DFT. However, there remains the issue of the accurate determination of the energy differences between states of different spin multiplicities, which is critical since these energy differences rule the phenomena of interest.

In order to address this issue, we first and foremost need highly accurate *ab initio* gas-phase data against which to straightforwardly and reliably assess the performances of the DFT methods, and thus bypass the need to resort to experimental data that posssibly strongly depend on environmental, temperature and pressure effects. Furthermore, these gas-phase reference data can be included in training data sets and may thus serve to develop improved semiempirical functionals. Coupled-cluster methods are the most accurate methods to treat electronic correlation in single-reference systems and, even in their standard formulation, they can be used to reliably deal with situations of multi-reference character [206-209].

In this respect, the CCSD(T) method [210] is considered the gold standard of quantum chemistry. We have therefore undertaken the determination of highly accurate estimates of the spin-state energy differences in benchmark complexes from the results of intensive scalar-relativistic CCSD(T) (SR-CCSD(T)) calculations performed on reference geometries and extrapolated to the complete basis set (CBS) limit.

For the HS-LS energy difference $\Delta E_{\mathrm{HL}}^{\mathrm{el}}$ in the benchmark complexes $[Fe(NCH)_6]^{2+}$ and $[Co(NCH)_6]^{2+}$ in D_{2d} symmetry, we have determined SR-CCSD(T)/CBS values of -712 cm^{-1} and -3111 cm^{-1}, respectively [211]. These results were then used to assess the performances of the CASPT2 second-order multi-reference perturbation theory (MRPT2) method, [212, 213] and of 30 functionals of the GGA [74, 75, 214-216], meta-GGA [217-220], global hybrid [221, 222], range-separated hybrid [223-230] and double-hybrid [231-233] types. For both complexes, $\Delta E_{\mathrm{HL}}^{\mathrm{el}}$ is underestimated by the CASPT2 method, as defined from the standard zeroth-order Hamiltonian with an ionization potential - electron affinity (IPEA) shift of 0.25 au [234]. The underestimation of $\Delta E_{\mathrm{HL}}^{\mathrm{el}}$ at the CASPT2 level for $[Fe(NCH)_6]^{2+}$ and other iron(II) complexes with a $[FeN_6]$ core was previously reported [235, 236]. This implies for $[Fe(bpy)_3]^{2+}$@Y that the estimate of $\Delta E_{\mathrm{HL}}^{\circ}[\mathrm{Y}] = 5400 \pm 1500$ cm^{-1} obtained from the combination of CASPT2 and DFT results [119, 162, 173] is actually a lower limit (see Section 3.2). At the DFT level, some functionals performed within chemical accuracy (± 1 kcal/mol $\approx \pm 350$ cm^{-1}) for the spin-state energetics of $[Fe(NCH)_6]^{2+}$ (X3LYP [237], CAM-B3LYP [229]), others for that of $[Co(NCH)_6]^{2+}$ (PBE0, M06 [238], mPW2-PLYP [231, 232]), but none of them performed so accurately for both complexes at the same time. Interestingly, for the CAM-PBE0 range-separated hybrid [230] characterized by a short-range exact-exchange contribution of $\alpha = 0.25$ and a range-separation parameter of $\omega = 0.30$ au^{-1} [230], we showed that, by slightly increasing α to 0.32 while slightly decreasing ω to 0.25 au^{-1}, one obtains a functional which performs simultaneously within chemical accuracy for the evaluation of $\Delta E_{\mathrm{HL}}^{\mathrm{el}}$ in both complexes [211].

This confirms that, thanks to the high flexibility of the functional forms, performing semiempirical functionals of broad applicability may be devised by including transition-metal spin-state energetics data in the training sets. We have enriched the data set with the results obtained for the spin-state energetics of the d^5 - d^7 $[M(NCH)_6]^{n+}$ complexes in D_{2d} (M = Mn, Fe, Co, Ni; $n = 2$ or 3), extending the study to the intermediate-spin states in the d^5 and d^6 complexes (to be published). Furthermore, to vary the coordination spheres of the transition metal ions and thus make the data set more comprehensive, we are extending the coupled-cluster study to the metalloporphyrins.

The availability of accurate benchmark data is also highly desirable because DFT methods can be used to accurately determine the spin-state energetics of complexes of a transition metal ion and of their compounds, provided that the spin-state energetics of one of these complexes are accurately known. This statement could be put on firm ground during the comparative DFT study of the complexes $[Co(NCH)_6]^{2+}$, $[Co(bpy)_3]^{2+}$ and $[Co(tpy)_2]^{2+}$, by considering the Born-Haber cycle of Fig. **10** [239].

The thermodynamic cycle shows that the change in the HS-LS Gibbs free energy differences of a complex upon a ligand exchange reaction:

$$\Delta(\Delta\mathcal{G}_{\mathrm{HL}})_{\mathrm{L}_a \to \mathrm{L}_b} = \Delta\mathcal{G}_{\mathrm{HL}}(\mathrm{L}_b) - \Delta\mathcal{G}_{\mathrm{HL}}(\mathrm{L}_a) \quad (6)$$

can be determined from the knowledge of the Gibbs free energy differences $\Delta_r\mathcal{G}_{\Gamma}(\mathrm{L}_a \to \mathrm{L}_b)$, ($\Gamma$ = LS, HS) associated to the $\mathrm{L}_a \to \mathrm{L}_b$ ligand substitutions in the two spin states, using the relation:

$$\Delta(\Delta\mathcal{G}_{\mathrm{HL}})_{\mathrm{L}_a \to \mathrm{L}_b} = \Delta_r\mathcal{G}_{\mathrm{HS}}(\mathrm{L}_a \to \mathrm{L}_b) - \Delta_r\mathcal{G}_{\mathrm{LS}}(\mathrm{L}_a \to \mathrm{L}_b) \quad (7)$$

which in the $T \to 0$ limit reduces to an identical equality between zero-point energy differences. It follows that the change in the spin-state energetics or in the thermodynamics of the LS $\leftrightarrows$ HS equilibrium of a complex upon a ligand exchange reaction can be accurately described by any functional able to describe the thermochemistry of the exchange reaction in the two spin states accurately. As discussed in Ref. [239], this tends to be the case for most modern functionals. The conclusion thus drawn can be readily extended to any chemical modifications which may also affect the outer coordination sphere, like for instance for $[Fe(bpy)_3]^{2+}$ upon encapsulation in the supercage of zeolite Y. For the Co(II) complexes, using the highly accurate *ab initio* estimate of the HS-LS energy difference in $[Co(NCH)_6]^{2+}$, best estimates of $\Delta E_{\mathrm{HL}}^{\circ}(\mathrm{bpy}) \approx -2800$ cm^{-1} and $\Delta E_{\mathrm{HL}}^{\circ}(\mathrm{tpy}) \approx 0$ cm^{-1} were obtained for $[Co(bpy)_3]^{2+}$ and $[Co(tpy)_2]^{2+}$, respectively [239]. These results agree well with the known magnetic behavior of the two complexes: $[Co(bpy)_3]^{2+}$ is usually a HS species and it can be turned into a spin-crossover complex only in tightly confining environments such as those provided by the supercages of zeolite Y [240-242] or by the cavities of three-dimensional oxalate networks [243, 244]. As for $[Co(tpy)_2]^{2+}$, it is a spin-crossover complex whose magnetic behavior is strongly sensitive to its environment [245-258].

In summary, the results obtained for the reparametrization of the CAM-PBE0 functional and those for the HS-LS energy differences in the Co(II) complexes hold

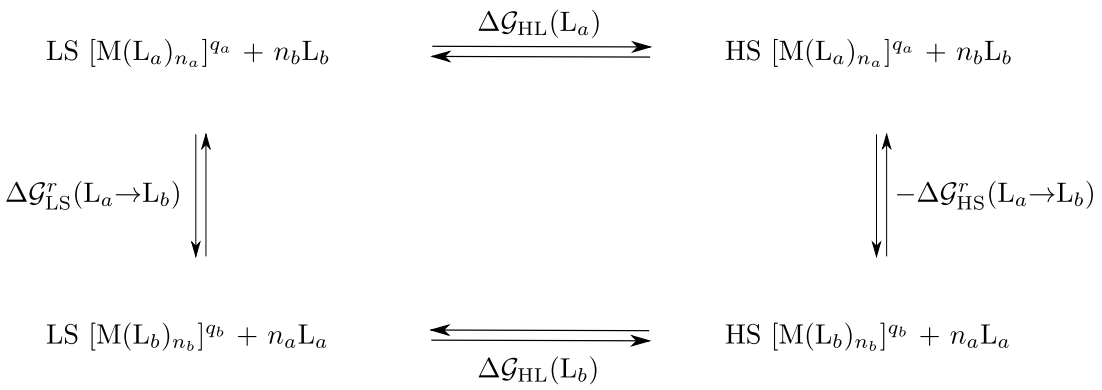

Fig. (10). Free energy "Born-Haber" cycle for the determination of the change $^{\Delta(\Delta\mathcal{G}_{\mathrm{HL}})_{\mathrm{L}_a\rightarrow\mathrm{L}_b}}$ in the HS-LS Gibbs free energy difference upon a ligand exchange reaction.

the promise that the spin-state energetics of a complex and the evolution of this one with the chemical nature of its ligands or with its environment can be accurately predicted within DFT.

CONFLICT OF INTEREST

The author confirms that this article content has no conflicts of interest.

ACKNOWLEDGEMENTS

Many coworkers, students and friends have helped in developing the ideas outlined in this review. I especially would like to thank Andreas Hauser, Mark Casida and Alfredo Vargas for their contributions. Helpful comments and stimulating discussions with Andreas Hauser while writing the manuscript are also acknowledged. This research is supported by grants from the Swiss National Supercomputing Centre (CSCS) under project IDs s103 and s296 and by the Center for Advanced Modeling Science (CADMOS) under project ID CTESIM.

REFERENCES

[1] Ksenofontov, V.; Gaspar, A.B.; Gütlich, P. In Spin Crossover in Transition Metal Compounds III ; Gütlich, P.; Goodwin, H.A.; Eds., *Top. Curr. Chem*., **2004**, *235*, 23-64.

[2] Hauser, A. In Spin Crossover in Transition Metal Compounds II ; Gütlich, P., Goodwin, H.A., Eds., *Top. Curr. Chem*., **2004**, Vol. *234*, 155-198.

[3] Spin Crossover in Transition Metal Compounds I; Gütlich, P.; Goodwin, H.A. Eds., Springer-Verlag: Heidelberg, **2004**.

[4] Spin Crossover in Transition Metal Compounds II; Gütlich, P.; Goodwin, H.A. Eds., Springer-Verlag: Heidelberg, **2004**.

[5] Spin Crossover in Transition Metal Compounds III; Gütlich, P.; Goodwin, H.A. Eds., Springer-Verlag: Heidelberg, **2004**.

[6] Gütlich, P.; Hauser, A.; Spiering, H. Thermal and Optical Switching of Iron(II) Complexes. *Angew. Chem. Int. Ed. Engl.,* **1994**, *33*, 2024-2054.

[7] Gütlich, P.; Goodwin, H.A. Spin Crossover - An Overall Persective. *Top. Curr. Chem.,* **2004**, *233*, 1-47.

[8] Garcia, Y.; Gütlich, P. Thermal Spin Crossover in Mn(II), Mn(III), Cr(II) and Co(III) Cordination Compounds. *Top. Curr. Chem.,* **2004**, *234*, 49-62.

[9] Hauser, A. In Spin Crossover in Transition Metal Compounds I ; Gütlich, P., Goodwin, H.A., Eds., *Top. Curr. Chem*., Springer-Verlag: Heidelberg, **2004**, Vol. *233*, 49-58.

[10] Hohenberg, P.; Kohn, W. Inhomogeneous Electron gas. *Phys. Rev.* **1964**, *136*, B864-B871.

[11] Kohn, W.; Sham, L.J. Self-Consistent Equations Including Exchange and Correlation Effects. *Phys. Rev.,* **1965**, *140*, A1133-A1138.

[12] Parr, R.G.; Yang, W. Density-Functional Theory of Atoms and Molecules; Oxford University Press: New York, **1989**.

[13] Dreizler, R.M.; Gross, E.K. U. Density Functional Theory; An Approach to the Quantum Many-Body Problem; Springer-Verlag: New York, **1990**.

[14] Koch, W.; Holthausen, M.C. A Chemist's Guide to Density Functional Theory; Wiley-VCH Verlag: Weinheim (Federal Republic of Germany), **2001**.

[15] Martin, R.M. Electronic Structure (Basic Theory and Practical Methods); Cambridge University Press: New York, **2004**.

[16] Perdew, J.P.; Schmidt, K. Jacob's ladder of density functional approximations for the exchange correlation energy. *AIP Conf. Proc.,* **2001**, *577*, 1-20.

[17] Arbuznikov, A. Hybrid exchange correlation functionals and potentials: Concept elaboration. *J. Struct. Chem*., **2007**, *48*, S1-S31.

[18] Kümmel, S.; Kronik, L. Orbital-dependent density functionals: Theory and applications. *Rev. Mod. Phys.,* **2008**, *80*, 3-60.

[19] Thakkar, A.J.; McCarthy, S.P. Toward improved density functionals for the correlation energy. *J. Chem. Phys.* **2009**, *131*, 134109.

[20] Casida, M.E. Time-dependent density-functional theory for molecules and molecular solids. *J. Mol. Struct. Theochem.,* **2009**, *914*, 3-18.

[21] Cohen, A.J.; Mori-Sánchez, P.; Yang, W. Challenges for Density Functional Theory. *Chem. Rev.,* **2012**, *112*, 289-320.

[22] Bolvin, A. d → d Spectrum and High-Spin/Low-Spin Competition in d^6 Octahedral Coordination Compounds: *ab initio* Study of Potential Energy Curves. *J. Phys. Chem.* A, **1998**, *102*, 7525-7534.

[23] Paulsen, H.; Duelund, L.; Winkler, H.; Toftlund, H.; Trautwein, A.X. Free Energy of Spin-Crossover Complexes Calculated with Density Functional Methods. *Inorg. Chem.,* **2001**, *40*, 2201-2204.

[24] Hauser, A. Excited-state lifetimes of $[Fe(bipy)_3]^{2+}$ and $[Fe(phen)_3]^{2+}$. *Chem. Phys. Lett.* **1990**, *173*, 507-512.

[25] Deisenroth, S.; Hauser, A.; Spiering, H.; Gütlich, P. Time integral and time differential Mössbauer measurements on $[^{57}Co/Mn(bipy)_3](PF_6)_2$. *Hyperfine Interact*., **1994**, *93*, 1573-1577.

[26] Schenker, S.; Hauser, A.; Wang, W.; Chan, I.Y. Matrix effects on the high-spin→low-spin relaxation in $[M_{1-x}Fe_x(bipy)_3](PF_6)_2$ (M =Cd, Mn and Zn, bpy =2,2'-bipyridine). *Chem. Phys. Lett.,* **1998**, *297*, 281-286.

[27] Vankó, G.; Nagy, S.; Homonnay, Z.; Vértes, A. Sterical effects of encapsulation on some cobalt complexes built up in zeolite Y - A Mössbauer emission spectroscopy study. *Hyperfine Interact.,* **2000**, *126*, 163-167.

[28] Hauser, A.; Amstutz, N.; Delahaye, S.; Sadki, A.; Schenker, S.; Sieber, R.; Zerara, M. Fine Tuning the Electronic Properties of $[M(bpy)_3]^{2+}$ Complexes by Chemical Pressure (M=Fe^{2+}, Ru^{2+}, Co^{2+}, bpy=2,2'-Bypridine). *Struct. Bond.,* **2004**, *106*, 81-96.

[29] Hauser, A.; Enachescu, C.; Lawson Daku, M.; Vargas, A.; Amstutz, N. Low temperature lifetimes of metastable high-spin states in spin-crossover and in low-spin compounds : the rule and exceptions to the rule. *Coord. Chem. Rev.,* **2006**, *250*, 1642-1652.

[30] Gawelda, W.; Cannizo A.; Pham, V.-T.; Benfatto, M.; Zaushitsyn, Y.; Kaiser, M.; Grolimund, D.; Johnson, S.L.; Abela, R.; Hauser, A.; Bressler, C.; Chergui, M. Structural Determination of a Short-Lived Excited Iron(II) Complex by Picosecond X-Ray Absorption Spectroscopy. *Phys. Rev. Lett.,* **2007**, *98*, 057401.

[31] Gawelda, W.; Cannizo, A.; Pham, V.-T.; van Mourik, F.; Bressler, C.; Chergui, M. Ultrafast Nonadiabatic Dynamics of $[Fe^{II}(bpy)_3]^{2+}$ in Solution. *J. Am. Chem. Soc.,* **2007**, *129*, 8199-8206.

[32] Bressler, C.; Milne, C.; Pham, V.-T.; ElNahhas, A.; van der Veen, R.M.; Gawelda, W.; Johnson, S.; Beaud, P.; Grolimund, D.; Kaiser, M.; Borca, C.N.; Ingold, G.; Abela, R.; Chergui, M. Femtosecond XANES Study of the Light-Induced Spin Crossover Dynamics in an Iron(II) Complex. *Science*, **2009**, *323*, 489-492.

[33] Gawelda, W.; Pham, V.-T.; van der Veen, R.M.; Grolimund, D.; Abela, R.; Chergui, M.; Bressler, C. Structural analysis of ultrafast extended x-ray absorption fine structure with subpicometer spatial resolution: Application to spin crossover complexes. *J. Chem. Phys.,* **2009**, *130*, 124520.

[34] Consani, C.; Prémont-Schwarz, M.; ElNahhas, A.; Bressler, C.; van Mourik, F.; Cannizzo, A.; Chergui, M. Vibrational Coherences and Relaxation in the High-Spin State of Aqueous $[Fe^{II}(bpy)_3]^{2+}$. *Angew. Chem. Int.,* Ed. **2009**, *48*, 7184-7187.

[35] Vankó, G.; Glatzel, P.; Pham, V.-T.; Abela, R.; Grolimund, D.; Borca, C.N.; Johnson, S.L.; Milne, C.J.; Bressler, C. Picosecond Time-Resolved X-Ray Emission Spectroscopy: Ultrafast Spin-State Determination in an Iron Complex. *Angew. Chem. Int.,* Ed. **2010**, *49*, 5910-5912.

[36] Decurtins, S.; Gütlich, P.; Köhler, C.P.; Spiering, H.; Hauser, A. Light-induced excited spin-state trapping in a transition-metal complex: The hexa-1-propyltetrazole-iron(II) tetrafluoroborate spin-crossover system. *Chem. Phys. Lett.,* **1984**, *105*, 1-4.

[37] Buhks, E.; Navon, G.; Bixon, M.; Jortner, J. Spin Conversion Process in Solutions. *J. Am. Chem. Soc.,* **1984**, *102*, 2918-2923.

[38] Hauser, A.; Vef, A.; Adler, P. Intersystem crossing dynamics in Fe(II) coordination compounds. *J. Chem. Phys.,* **1991**, *95*, 8710-8717.

[39] Lawson Daku, L.M.; Vargas, A.; Hauser, A.; Fouqueau, A.; Casida, M.E. Assessment of Density Functionals for the High-Spin/Low-Spin Energy Difference in the Low-Spin Iron(ii)Tris(2,2'-bipyridine) Complex. *ChemPhysChem* **2005**, *6*, 1393-1410.

[40] Gunnarsson, O.; Lundqvist, B.I. Exchange and correlation in atoms, molecules, and solids by the spin-density-functional formalism. *Phys. Rev. B,* **1976**, *13*, 4274-4298.

[41] Görling, A. Symmetry in density-functional theory. Phys. Rev. A **1993**, *47*, 2783-2799.

[42] Kaplan, I.G. Problems in DFT with the total spin and degenerate states. *Int. J. Quantum Chem*. **2007**, *107*, 2595-2603.

[43] Perdew, J.P.; Ruzsinszky, A.; Constantin, L.A.; Sun, J.; Csonka, G.I. Some Fundamental Issues in Ground-State Density Functional Theory: A Guide for the Perplexed. *J. Chem. Theory Comput.* **2009**, *5*, 902-908.

[44] Jacob, C.R.; Reiher, M. Spin in Density-Functional Theory. *Int. J. Quantum Chem.,* **2012**, *112*, 3661-3684.

[45] Della Sala, F.; Görling, A. Open-shell localized Hartree-Fock approach for an efficient effective exact-exchange Kohn-Sham treatment of open-shell atoms and molecules. *J. Chem. Phys.,* **2003**, 118, 10143.

[46] Görling, A. Orbital- and state-dependent functionals in density-functional theory. *J. Chem. Phys.,* **2005**, *123*, 062203.

[47] Theophilou, A.K. Density Functional Theory for Excited States and Special Symmetries. *Int. J. Quantum Chem.,* **1997**, *61*, 333-340.

[48] Nagy, A.; Liu, S.; Bartolloti, L. Generalized density functional theory for degenerate states. *J. Chem. Phys.,* **2005**, *122*, 134107.

[49] Daul, C. Density functional theory applied to the excited states of coordination compounds. *Int. J. Quantum Chem.,* **1994**, *52*, 867-877.

[50] Ziegler, T.; Rauk, A.; Baerends, E.J. Multiplet energies; Calculation by the Hartree-Fock-Slater method. *Theor. Chim. Acta,* **1977**, *43*, 261-271.

[51] Noodleman, L.; Norman, Jr., J.G. The Xα valence bond theory of weak electronic coupling. Application to the low-lying states of $Mo_2Cl_8^{4-}$, *J. Chem. Phys.,* **1979**, *70*, 4903-4906.

[52] Noodleman, L. Valence bond description of antiferromagnetic coupling in transition metal dimers. *J. Chem. Phys.,* **1981**, *74*, 5737-5743.

[53] Daul, C.A.; Doclo, K.G.; Stükl, A.C. In Recent Advances in Density Functional Methods. Part II ; Chong, D.P., Ed.; Recent Advances in Computational Chemistry; World Scientific: Singapore, **1997**; Vol. *1*; pp 61-115.

[54] Ciofini, I.; Daul, C.A. DFT calculations of molecular magnetic properties of coordination compounds. *Coord. Chem. Rev.,* **2003**, *238-239*, 187-209.

[55] Fouqueau, A.; Mer, S.; Casida, M.E.; Lawson Daku, L.M.; Hauser, A.; Mineva, T. Comparison of density functionals for energy and structural differences between the high-[$^5T_{2g}$: $(t_{2g})^4(e_g)^2$] and low-[$^1T_1$: $(t_{2g})^6(e_g)^0$] spin states of the hexaquoferrous cation $[Fe(H_2O)_6]^{2+}$. *J. Chem. Phys.,* **2004**, *120*, 9473-9486.

[56] Caballol, R.; Castell, O.; Illas, F.; de P.R. Moreira, I.; Malrieu, J.P. Remarks on the Proper Use of the Broken Symmetry Approach to Magnetic Coupling. *J. Phys. Chem.* A, **1997**, *101*, 7860-7866.

[57] Mouesca, J.-M. Quantitative harmonization of the three molecular orbital, valence bond, and broken symmetry approaches to the exchange coupling constant: Corrections and discussion. *J. Chem. Phys.,* **2000**, *113*, 10505-10511.

[58] Lawson Daku, L.M.; Borshch, S.A.; Robert, V.; Bigot, B. Magnetostructural correlations and spin model of $(VO)_2P_2O_7$. *Phys. Rev. B,* **2001**, *63*, 174439.

[59] Lovell, T.; Himo, F.; Han, W.-G.; Noodleman, L. Density functional methods applied to metalloenzymes. *Coord. Chem. Rev.,* **2003**, *238-239*, 211-232.

[60] Noodleman, L.; Lovell, T.; Liu, T.; Himo, F.; Torres, R.A. Insights into properties and energetics of iron-sulfur proteins from simple clusters to nitrogenase. *Curr. Opin. Chem. Biol.,* **2002**, *6*, 259-273.

[61] de P.R. Moreira, I.; Illas, F. A unified view of the theoretical description of magnetic coupling in molecular chemistry and solid state physics. *Phys. Chem. Chem. Phys.,* **2006**, *8*, 1645-1659.

[62] Bencini, A.; Totti, F. A Few Comments on the Application of Density Functional Theory to the Calculation of the Magnetic Structure of Oligo-Nuclear Transition Metal Clusters. *J. Chem. Theory Comput.,* **2009**, *5*, 144-154.

[63] Monari, A.; Maynau, D.; Malrieu, J.-P. Determination of spin Hamiltonians from projected single reference configuration interaction calculations.I. Spin 1/2 systems. *J. Chem. Phys.,* **2010**, *133*, 044106.

[64] Cramer, C.J.; Truhlar, D.G. Density functional theory for transition metals and transition metal chemistry. *Phys. Chem. Chem. Phys.,* **2009**, *11*, 10757-10816.

[65] Gräfenstein, J.; Kraka, E.; Filatov, M.; Cremer, D. Can Unrestricted Density-Functional Theory Describe Open Shell Singlet Biradicals. *Int. J. Mol. Sci.,* **2002**, *3*, 360-394.

[66] Lawson Daku, L.M.; Linares, J.; Boillot, M.-L. Ab initio static and molecular dynamics study of 4-styrylpyridine: Structure, energy and reactivity of the cis and trans isomers in the ground state. *ChemPhysChem* **2007**, *8*, 1402-1416.

[67] Filatov, M.; Shaik, S. Spin-restricted density functional approach to the open-shell problem. *Chem. Phys. Lett.,* **1998**, *288*, 689-697.

[68] Filatov, M.; Shaik, S. A spin-restricted ensemble-referenced Kohn-Sham method and its application to diradicaloid situations. *Chem. Phys. Lett.,* **1999**, *304*, 429-437

[69] Illas, F.; de P.R. Moreira, I.; Bofill, J.M.; Filatov, M. Spin Symmetry Requirements in Density Functional Theory: The Proper Way to Predict Magnetic Coupling Constants in Molecules and Solids. *Theor. Chem. Acc.,* **2006**, *116*, 587-597.

[70] de P.R. Moreira, I.; Costa, R.; Filatov, M.; Illas, F. Restricted Ensemble-Referenced Kohn-Sham versus Broken Symmetry Approaches in Density Functional Theory: Magnetic Coupling in Cu Binuclear Complexes. *J. Chem. Theory Comput.,* **2007**, *3*, 764-774.

[71] Huix-Rotllant, M.; Filatov, M.; Gozem, S.; Schapiro, I.; Olivucci, M.; Ferré, N. Assessment of Density Functional Theory for Describing the Correlation Effects on the Ground and Excited State Potential Energy Surfaces of a Retinal Chromophore Model. *J. Chem. Theory Comput.,* **2013**, 9, 3917-3932.

[72] Görling, A. Proper Treatment of Symmetries and Excited States in a Computationally Tractable Kohn-Sham Method. *Phys. Rev. Lett.,* **2000**, *85*, 4229-4232.

[73] Ullrich, C.A.; Kohn, W. Kohn-Sham Theory for Ground-State Ensembles. *Phys. Rev. Lett.,* **2001**, *87*, 093001.

[74] Becke, A.D. Density-functional exchange energy approximation with correct asymptotic behavior. *Phys. Rev. A,* **1988**, *38*, 3098-3100.

[75] Perdew, J.P. Density-functional approximation for the correlation energy of the in homogeneous gas. *Phys. Rev. B,* **1986**, *33*, 8822-8824.

[76] Perdew, J.P. Erratum: Density-functional approximation for the correlation energy of the inhomogeneous gas. *Phys. Rev. B,* **1986**, *34*, 7406.

[77] Perdew, J.P.; Chevary, J.A.; Vosko, S.H.; Jackson, K.A.; Pederson, M.R.; Singh, D.J.; Fiolhais, C. Atoms, molecules, solids, and surfaces: Applications of the generalized gradient approximation for exchange and correlation. *Phys. Rev. B,* **1992**, *46*, 6671-6687.

[78] Perdew, J.P.; Chevary, J.A.; Vosko, S.H.; Jackson, K.A.; Pederson, M.R.; Singh, D.J.; Fiolhais, C. Erratum: Atoms, molecules, solids, and surfaces: Applications of the generalized gradient approximation for exchange and correlation [*Phys. Rev. B, 47*, 6671 (**1992**)]. *Phys. Rev. B,* **1993**, *48*, 4978.

[79] Perdew, J.P.; Burke, K.; Wang, Y. Generalized gradient approximation for the exchange-correlation hole of a many-electron system. *Phys. Rev. B,* **1996**, *54*, 16533-16539.

[80] Perdew, J.P.; Burke, K.; Wang, Y. Erratum: Generalized gradient approximation for the exchange-correlation hole of a many-electron system [*Phys. Rev. B, 54*, 16533 (**1996**)]. *Phys. Rev. B,* **1998**, *57*, 14999.

[81] Perdew, J.P.; Burke, K.; Ernzerhof, M. Generalized Gradient Approximation Made Simple. *Phys. Rev. Lett.,* **1996**, *77*, 3865-3868.

[82] Perdew, J.P.; Burke, K.; Ernzerhof, M. Erratum: Generalized Gradient Approximation Made Simple [*Phys. Rev. Lett., 77*, 3865 (**1996**)]. *Phys. Rev. Lett.,* **1997**, 78, 1396.

[83] Hammer, B.; Hansen, L.B.; Nørskov, J.K. Improved adsorption energetics within density-functional theory using revised Perdew-Burke-Ernzerhof functionals. *Phys. Rev. B,* **1999**, *59*, 7413-7421.

[84] Gaussian NEWS, v. 5, no. 2, summer **1994**, p. 2. "Becke3LYP Method References and General Citation Guidelines".

[85] Reiher, M.; Salomon, O.; Hess, B.A. Reparameterization of hybrid functionals based on energy differences of state of different multiplicity. *Theor. Chem. Acc.,* **2001**, *107*, 48-55.

[86] Reiher, M. Theoretical Study of the $Fe(phen)_2(NCS)_2$ Spin-Crossover Complex with Reparametrized Density Functionals. *Inorg. Chem.* **2002**, *41*, 6928-6935.

[87] Salomon, O.; Reiher, M.; Hess, B.A. Assertion and validation of the performance of the B3LYP* functional for the first transition metal row and the G2 test set. *J. Chem. Phys.,* **2002**, *117*, 4729-4737.

[88] Perdew, J.P.; Ernzerhof, M.; Burke, K. Rationale for mixing exact exchange with density functional approximations. *J. Chem. Phys.,* **1996**, *105*, 9982-9985.

[89] Adamo, C.; Barone, V. Toward reliable density functional methods without adjustable parameters: The PBE0 model. *J. Chem. Phys.,* **1999**, *110*, 6158-6170.

[90] Renz, F.; Oshio, H.; Spiering, H.; Ksenofotnov, V.; Waldeck, M.; Spiering, H.; Gütlich, P. Strong Field Iron(II) Complex Converted by Light into a Long-Lived High-Spin State. *Angew. Chem. Int.,* Ed. **2000**, *39*, 3699-3700.

[91] Oshio, H.; Spiering, H.; Ksenofontov, V.; Renz, F.; Gütlich, P. Electronic Relaxation Phenomena Following $^{57}Co(EC)^{57}Fe$ Nuclear Decay in $[Mn^{II}(terpy)_2](ClO_4)_2{\cdot}1/2H_2O$ and in the Spin Crossover Complexes $[Co^{II}(terpy)_2]X_2{\cdot}nH_2O$ (X =Cl and ClO_4): A Mössbauer Emission Spectroscopic Study. *Inorg. Chem.,* **2001**, *40*, 1143-1150.

[92] Ceperley, D.M.; Adler, B.J. Ground State of the Electron Gas by a Stochastic Method. *Phys. Rev. Lett.,* **1980**, *45*, 566-569.

[93] Vosko, S.H.; Wilk, L.; Nusair, M. Accurate Spin-Dependent Electron Liquid Correlation Energies for Local Spin Density Calculations: A Critical Analysis. *Can. J. Phys.,* **1980**, *58*, 1200-1211.

[94] Wang, Y.; Perdew, J.P. Correlation hole of the spin-polarized gas, with exact small wave-vector and high-density scaling. *Phys. Rev. B,* **1991**, *44*, 13298-13307.

[95] Perdew, J.P.; Wang, Y. Accurate and simple analytic representation of the electron gas correlation energy. *Phys. Rev. B,* **1992**, *45*, 13244-13249.

[96] Dirac, P.A.M. Quantum Mechanics of Many-Electron Systems. *Proc. R. Soc. Lond.* A, **1929**, *123*, 714-733.

[97] Slater, J.C. A Simplification of the Hartree-Fock Method. *Phys. Rev.,* **1951**, *81*, 385-390.

[98] Paulsen, H.; Trautwein, A.X. In Spin Crossover in Transition Metal Compounds II ; Gütlich, P., Goodwin, H.A., Eds.; *Top. Curr. Chem*., **2004**; *235*, 197-219.

[99] Brehm, G.; Reiher, M.; Schneider, S. Estimation of the Vibrational Contribution to the Entropy Change Associated with the Low- to High-Spin Transition in $Fe(phen)_2(NCS)_2$ Complexes: Results Obtained by IR and Raman Spectroscopy and DFT Calculations. *J. Phys. Chem*. A, **2002**, *106*, 12024-12034.

[100] Perdew, J.P.; Kurth, S. In a primer in density functional theory; Fiolhais, C., Nogueira, F., Marques, M., Eds.; *Lecture Notes in Physics*; **2003**; Vol. *620*; pp 1-55.

[101] Zupan, A.; Burke, K.; Ernzerhof, M.; Perdew, J.P. Distributions and averages of electron density parameters: Explaining the effects of gradient corrections. *J. Chem. Phys.,* **1997**, *106*, 10184-10293.

[102] Ghosh, A.; Taylor, P.R. High-level ab initio calculations on the energetics of low-lying spin states of biologically relevant transition metal complexes: a first progress report. *Curr. Opin. Chem. Biol.,* **2003**, *7*, 113-124.

[103] Harvey, J.N.; Poli, R.; Smith, K.M. Understanding the reactivity of transition metal complexes involving multiple spin states. *Coord. Chem. Rev.,* **2003**, *238-239*, 347-361.

[104] Deeth, R.J.; Fey, N. The Performance of Nonhybrid Density Functionals for Calculating the Structure and Spin States of Fe(II) and Fe(III) Complexes. *J. Comput. Chem.,* **2004**, *25*, 1840-1848.

[105] Kaltsoyannis, N.; McGrady, J.; Harvey, J. Principles and Applications of Density Functional Theory in Inorganic Chemistry I ; Structure & Bonding; Springer Berlin/Heidelberg, **2004**; Vol. *112*; pp 81-102.

[106] Swart, M.; Groenhof, A.R.; Ehlers, A.W.; Lammertsma, K. Validation of Exchange-Correlation Functionals for Spin States of Iron Complexes. *J. Phys. Chem. A,* **2004**, *108*, 5479-5483.

[107] Ganzenmüller, G.; Berkaïne, N.; Fouqueau, A.; Casida, M.E.; Reiher, M. Comparison of density functionals for differences between the high-($^5T_{2g}$) and low-($^1A_{1g}$) spin states of iron(II) compounds. IV. Results for the ferrous complexes [Fe(L)('NHS_4')]. *J. Chem. Phys.,* **2005**, *122*, 234321.

[108] Smith, D.M.A.; Dupuis, M.; Straatsma, T.P. Multiplet splittings and other properties from density functional theory: an assessment in iron-porphyrin systems. *Molec. Phys.,* **2005**, *103*, 273-278.

[109] Fouqueau, A.; Casida, M.E.; Lawson Daku, L.M.; Hauser, A.; Neese, F. Comparison of density functionals for energy and structural differences between the high-[$^5T_{2g}$: $(t_{2g})^4(e_g)^2$] and low-[$^1T_1$: $(t_{2g})^6(e_g)^0$] spin states of iron(II) coordination compounds: II. Comparison of results for more than ten modern functionals with ligand field theory and ab initio results for the hexaquoferrous cation $[Fe(H_2O)_6]^{2+}$, and the hexaminoferrous cation $[Fe(NH_3)_6]^{2+}$. *J. Chem. Phys.,* **2005**, *122*, 044110.

[110] Ghosh, A. Transition metal spin state energetics and noninnocent systems: challenges for DFT in the bioinorganic arena. *J. Biol. Inorg. Chem.,* **2006**, *11*, 712-724.

[111] Vargas, A.; Zerara, M.; Krausz, E.; Hauser, A.; Lawson Daku, L.M. Density-functional investigation of the geometric, energetic and optical properties of the cobalt(II)tris(2,2'-bipyridine) complex in the high-spin and in the Jahn-Teller unstable low-spin states. *J. Chem. Theory Comput.,* **2006**, 2, 1342-1359.

[112] Scherlis, D.A.; Cococcioni, M.; Sit, P.; Marzari, N. Simulation of Heme Using DFT+U: A Step toward Accurate Spin-State Energetics. *J. Phys. Chem. B,* **2007**, *111*, 7384-7391.

[113] Guillon, T.; Salmon, L.; Molnár, G.; Zein, S.; Borshch, S.; Bousseksou, A. Investigation of the Two-Step Spin Crossover Complex Fe[5-NO_2-sal-(1,4,7,10)] Using Density Functional Theory.*J. Phys. Chem. A,* **2007**, *111*, 8223-8228.

[114] Zein, S.; Borshch, S.A.; Fleurat-Lessard, P.; Casida, M.E.; Chermette, H. Assessment of the exchange-correlation functionals for the physical description of spin transition phenomena by density functional theory methods: All the same? *J. Chem. Phys.,* **2007**, *126*, 014105.

[115] Tangen, E.; Conradie, J.; Ghosh, A. Bonding in Low-Coordinate Environments: Electronic Structure of Pseudotetrahedral Iron-Imido Complexes. *J. Chem. Theory Comput.,* **2007**, *3*, 448-457.

[116] Conradie, J.; Ghosh, A. Electronic Structure of Trigonal-Planar Transition-Metal-Imido Complexes: Spin-State Energetics, Spin-Density Profiles, and the Remarkable Performance of the OLYP Functional. *J. Chem. Theory Comput*., **2007**, *3*, 689-702.

[117] Wasbotten, I.H.; Ghosh, A. Spin-State Energetics and Spin-Crossover Behavior of Pseudotetrahedral Cobalt(III)-Imido Complexes. The Role of the Tripodal Supporting Ligand. *Inorg. Chem.,* **2007**, *46*, 7890-7898.

[118] Conradie, J.; Wondimagegn, T.; Ghosh, A. Spin States at a Tipping Point: What Determines the $d^1_{z^2}$ Ground State of Nickel(III) Tetra(^{t}butyl)porphyrin Dicyanide? *J. Phys. Chem. B,* **2008**, *112*, 1053-1056.

[119] Pierloot, K.; Vancoillie, S. Relative energy of the high-($^5T_{2g}$) and low-($^1A_{1g}$) spin states of the ferrous complexes [Fe(L)(NHS_4)]: CASPT2 versus density functional theory. *J. Chem. Phys.,* **2008**, *128*, 034104.

[120] Marti, K.H.; Ondík, I.M.; Moritz, G.; Reiher, M. Density matrix renormalization group calculations on relative energies of transition metal complexes and clusters. *J. Chem. Phys.,* **2008**, *128*, 014104.

[121] Jensen, K.P. Bioinorganic Chemistry Modeled with the TPSSh Density Functional. *Inorg. Chem.,* **2008**, *47*, 10357-10365.

[122] Swart, M. Accurate Spin-State Energies for Iron Complexes. *J. Chem. Theory Comput.,* **2008**, *4*, 2057-2066.

[123] Rotzinger, F.P. Investigation of the Ligand-Field States of the Hexaammine Cobalt(III) Ion with Quantum Chemical Methods. *J. Chem. Theory Comput.,* **2009**, *5*, 1061-1067.

[124] Jensen, K.P.; Cirera, J. Accurate Computed Enthalpies of Spin Crossover in Iron and Cobalt Complexes. *J. Phys. Chem. A,* **2009**, *113*, 10033-10039.

[125] Oláh, J.; Harvey, J.N. NO Bonding to Heme Groups: DFT and Correlated *ab Initio* Calculations. *J. Phys. Chem. A,* **2009**, *113*, 7338-7345.

[126] Ye, S.; Neese, F. Accurate Modeling of Spin-State Energetics in Spin-Crossover Systems with Modern Density Functional Theory. *Inorg. Chem*., **2010**, *49*, 772-774.

[127] Zhao, H.; Pierloot, K.; Langner, E.H.G.; Swarts, J.C.; Conradie, J.; Ghosh, A. Low-Energy States of Manganese-Oxo Corrole and Corrolazine: Multiconfiguration Reference *ab Initio* Calculations. *Inorg. Chem*., **2012**, *51*, 4002-4006.

[128] Monat, J.E.; McCusker, J.K. Femtosecond Excited-State Dynamics of an Iron(II) Polypyridyl Solar Cell Sensitizer Model. *J. Am. Chem. Soc.,* **2000**, *122*, 4092-4097.

[129] Brady, C.; Callaghan, P.L.; Ciunik, Z.; Coates, C.G.; Døssing, A.; Hazell, A.; Mc-Garvey, J.J.; Schenker, S.; Toftlund, H.; Trautwein, A.X.; Winkler, H.; Wolny, J.A. Molecular Structure and Vibrational Spectra of Spin-Crossover Complexes in Solution and Colloidal Media: Resonance Raman and Time-Resolved Resonance Raman Studies. *Inorg. Chem.,* **2004**, *43*, 4289-4299.

[130] Juban, E.A.; Smeigh, A.L.; Monat, J.E.; McCusker, J.K. Ultrafast dynamics of ligand-field excited states. *Coord. Chem. Rev.,* **2006**, *250*, 1783-1791.

[131] Smeigh, A.L.; Creelman, M.; Mathies, R.A.; McCusker, J.K. Femtosecond Time-Resolved Optical and Raman Spectroscopy of Photoinduced Spin Crossover: Temporal Resolution of Low-to-High Spin Optical Switching. *J. Am. Chem. Soc.,* **2008**, *130*, 14105-14107.

[132] Wolf, M.M.N.; R. Groß, C.S.; Wolny, J.A.; Schünemann, V.; Døssing, A.; Paulsen, H.; McGarvey, J.J.; Diller, R. Subpicosecond time resolved infrared spectroscopy of high-spin state formation in Fe(II) spin crossover complexes. *Phys. Chem. Chem. Phys.,* **2008**, *10*, 4264-4273.

[133] Huse, N.; Kim, T.K.; Jamula, L.; McCusker, J.K.; de Groot, F.M. F.; Schoenlein, R.W. Photo-Induced Spin-State Conversion in Solvated Transition Metal Complexes Probed via Time-Resolved Soft X-ray Spectroscopy. *J. Am. Chem. Soc*., **2010**, *132*, 6809-6816.

[134] Huse, N.; Cho, H.; Hong, K.; Jamula, L.; de Groot, F.M.F.; Kim, T.K.; Mc-Cusker, J.K.; Schoenlein, R.W. Femtosecond Soft X-ray Spectroscopy of Solvated Transition-Metal Complexes: Deciphering the Interplay of Electronic and Structural Dynamics. *J. Phys. Chem. Lett*., **2011**, *2*, 880-884.

[135] Haldrup, K.; Vankó, G.; Gawelda, W.; Galler, A.; Doumy, G.; March, A.M.; Kanter, E.P.; Bordage, A.; Dohn, A.; van Driel, T.B.; Kjær, K.S.; Lemke, H.T.; Canton, S.E.; Uhlig, J.; Sundström, V.; Young, L.; Southworth, S.H.; Nielsen, M.M.; Bressler, C. Guest-Host Interactions Investigated by Time-Resolved X-ray Spectroscopies and Scattering at MHz Rates: Solvation Dynamics and Photoinduced Spin Transition in Aqueous $Fe(bipy)_3^{2+}$. *J. Phys. Chem. A,* **2012**, *116*, 9878-9887.

[136] Lawson Daku, L.M.; Hauser, A. Ab Initio Molecular Dynamics Study of an Aqueous Solution of $[Fe(bpy)_3)(Cl]_2$ in the Low-Spin and in the High-Spin State. *J. Phys. Chem. Lett.,* **2010**, *1*, 1830-1835.

[137] Car, R.; Parrinello, M. Unified Approach for Molecular Dynamics and Density-Functional Theory. *Phys. Rev. Lett.,* **1985**, *55*, 2471-2474.

[138] Marx, D.; Hutter, J. In Modern Methods and Algorithms of Quantum Chemistry, 2nd ed.; Grotendorst, J., Ed.; NIC series; John von Neumann Institute for Computing: Forschungszentrum Jülich, Germany, **2000**; Vol. *3*; pp 329-477.

[139] Lee, C.; Yang, W.; Parr, R.G. Development of the Colle-Salvetti correlation-energy formula into a functional of the electron density. *Phys. Rev. B,* **1988**, *37*, 785-789.

[140] Moret, M.-E.; Tavernelli, I.; Röthlisberger, U. Combined QM/MM and Classical Molecular Dynamics Study of $[Ru(bpy)_3]^{2+}$ in Water. *J. Phys. Chem., B* **2009**, *113*, 7737-7744.

[141] Richards, T.W. A brief history of the investigation of internal pressures. *Chem. Rev.,* **1925**, *2*, 315-348.

[142] Nishikiori, S.; Yoshikawa, H.; Sano, Y.; Iwamoto, T. Inorganic-Organic Hybrid Molecular Architectures of Cyanometalate Host and Organic Guest Systems: Specific Behavior of the Guests. *Acc. Chem. Res.,* **2005**, *38*, 227-234.

[143] Sugi, M.; Matsumoto, Y.; Kimura, N.; Komatsubara, T.; Aoki, H.; Terashima, T.; Uji, S. Fermi Surface Properties of $CeRu2(Si_{1-x}Ge_x)_2$ in Magnetic Fields above the Metamagnetic Transitions. *Phys. Rev. Lett.,* **2008**, *101*, 056401.

[144] Espallargas, G.M.; Brammer, L.; Allan, D.R.; Pulham, C.R.; Robertson, N.; Warren, J.E. Noncovalent Interactions under Extreme Conditions: High-Pressure and Low-Temperature Diffraction Studies of the Isostructural Metal-Organic Networks (4-Chloropyridinium)$_2$[CoX_4] (X =Cl, Br). *J. Am. Chem. Soc.,* **2008**, *130*, 9058-9071.

[145] Kiswandhi, A.; Brooks, J.S.; Lu, J.; Whalen, J.; Siegrist, T.; Zhou, H.D. Chemical pressure effects on structural, magnetic, and transport properties of $Mn_{1-x}Co_xV_2O_4$. *Phys. Rev. B,* **2011**, *84*, 205138.

[146] Sampathkumaran, E.V.; Dhar, S.K.; Malik, S.K. Investigation of chemical pressure effects on the magnetic behaviour of $CeRh_2Si_2$. *J. Phys. C: Solid State Phys.,* **1987**, *20*, L53-L56.

[147] Lawson Daku, L.M.; Hagemann, H. First-principles study of the pressure dependence of the structural and vibrational properties of the ternary metal hydride Ca_2RuH_6. *Phys. Rev. B,* **2007**, *76*, 014118.

[148] Estephane, J.; Groppo, E.; Damin, A.; Vitillo, J.G.; Gianolio, D.; Lamberti, C.; Bordiga, S.; Prestipino, C.; Nikitenko, S.; Quadrelli, E.A.; Taoufik, M.; Basset, J.M.; Zecchina, A. Structure and Enhanced Reactivity of Chromocene Carbonyl Confined inside Cavities of NaY Zeolite. *J. Phys. Chem. C,* **2009**, *113*, 7305-7315.

[149] Chrétien, M.N. Supramolecular photochemistry in zeolites: From catalysts to sunscreens. *Pure Appl. Chem*., **2007**, *79*, 1-20.

[150] McMorn, P.; Hutchings, G.J. Heterogeneous enantioselective catalysts: strategies for the immobilisation of homogeneous catalysts. *Chem. Soc. Rev.,* **2004**, *33*, 108-122.

[151] Gol'tsov, Y.G. Synthesis and properties of inclusion compounds: Zeolites containing encapsulated transition-metal complexes. *Theor. Exp. Chem*., **1999**, *35*, 183-197.

[152] Bedioui, F. Zeolite-encapsulated and clay-intercalated metal porphyrin, phthalocyanine and Schiff-base complexes as models for biomimetic oxidation catalysts: an overview. *Coord. Chem. Rev.,* **1995**, *144*, 39-68.

[153] Ozin, G.A.; Gil, C. Intrazeolite Organometallics and Coordination Complexes: Internal versus External Confinement of Metal Guests. *Chem. Rev.,* **1989**, *89*, 1749-1764.

[154] Payra, P.; Dutta, P.K. In Handbook of Zeolite Science and Technology; Auerbach, S.M., Carrado, K.A., Dutta, P.K., Eds.*; Marcel Dekker Publishing: New York*, **2003**; pp 1-19.

[155] DeWilde, W.; Peeters, G.; Lunsford, J.H. Synthesis and Spectroscopic Properties of Tris(2,2'-bipyridine)ruthenium(II) in Zeolite Y. *J. Phys. Chem.,* **1980**, *84*, 2306-2310.

[156] Herron, N. A Cobalt Oxygen Carrier in Zeolite Y. A Molecular "Ship in a Bottle". *Inorg. Chem.,* **1986**, *25*, 4714-4717.

[157] Quayle, W.H.; Peeters, G.; De Roy, G.L.; Vansant, E.F.; Lunsford, J.H. Synthesis and Spectroscopic Properties of Divalent and Trivalent Tris(2,2'-dipyridine)iron Complexes in Zeolite Y. *Inorg. Chem.,* **1982**, *21*, 2226-2231.

[158] Umemura, Y.; Minai, Y.; Tominaga, T. Evidence for Distortion in $[FeL_3]^{2+}$ (L =en, amp, bpy, phen) in a Y-type Zeolite. *J. Chem. Soc. Chem. Commun.* **1993**, 1822-1823.

[159] Vankó, G.; Homonnay, Z.; Nagy, S.; Vértes, A.; Pál-Borbély, G.; Beyer, H.K. On the synthesis and steric distortion of the tris(2,2-

bipyridine)iron(ii)complex ion in zeolite-Y. *Chem. Commun.,* **1996**, 785-786.

[160] Umemura, Y.; Minai, Y.; Tominaga, T. Structural Distortion of 6-Coordinated Fe(II) Complexes in Zeolite Y. *J. Phys. Chem. B,* **1999**, *103*, 647-652.

[161] Vijayalakshmi, R.; Kulshreshtha, S.K. Study of $[Fe^{II}(bpy)_3]^{2+}$ Complex Encapsulated in Zeolite Y. *Microp. Mesop. Mater.,* **2008**, *111*, 449-454.

[162] Vargas, A.; Hauser, A.; Lawson Daku, L.M. Influence of Guest-Host Interactions on the Structural, Energetic, and Mössbauer Spectroscopy Properties of Iron(II)tris(2,2'-bipyridine) in the Low-Spin and High-Spin States: A Density-Functional Theory Study of the Zeolite-Y Embedded Complex. *J. Chem. Theory Comput*., **2009**, *5*, 97-115.

[163] Boese, A.D.; Handy, N.C. A new parametrization of exchange-correlation generalized gradient approximation functionals. *J. Chem. Phys.,* **2001**, *114*, 5497-5503.

[164] Handy, N.C.; Cohen, A.J. Left-right correlation energy. *Molec. Phys.,* **2001**, *99*, 403-412.

[165] Mössbauer, R.L. Kernresonanzfluoreszenz von Gammastrahlung in Ir^{191}. Z. *Physik A,* **1958**, *151*, 124-143.

[166] Gütlich, P., Bill, E., Trautwein, A.X., Eds. Mössbauer Spectroscopy and Transition Metal Chemistry - Fundamentals and Applications*; Springer: Berlin*, **2011**.

[167] Neese, F.; Petrenko, T. In Mössbauer Spectroscopy and Transition Metal Chemistry - Fundamentals and Applications; Gütlich, P., Bill, E., Trautwein, A.X., Eds.; *Springer:Berlin,* **2011**; pp 137-199.

[168] Kurian, R.; Filatov, M. Calibration of ^{57}Fe isomer shift from ab initio calculations: Can theory and experiment reach an agreement? *Phys. Chem. Chem. Phys.,* **2010**, *12*, 2758-2762.

[169] Kurian, R.; Filatov, M. DFT Approach to the Calculation of Mossbauer Isomer Shifts. *J. Chem. Theory Comput*., **2008**, *4*, 278-285.

[170] Han, W.-G.; Liu, T.; Lovell, T.; Noodleman, L. DFT Calculations of ^{57}Fe Mössbauer Isomer Shifts and Quadrupole Splittings for Iron Complexes in Polar Dielectric Media: Applications to Methane Monooxygenase and Ribonucleotide Reductase. *J. Comput. Chem.,* **2006**, *27*, 1292-1306.

[171] Paulsen, H.; Schünemann, V.; Trautwein, A.X.; Winkler, H. Mössbauer studies of coordination compounds using synchrotron radiation. *Coord. Chem. Rev.* **2005**, *249*, 255-272.

[172] Neese, F. Quantum chemical calculations of spectroscopic properties of metalloproteins and model compounds: EPR and Mössbauer properties. *Curr. Opin. Chem. Biol.,* **2003**, *7*, 125-135.

[173] Pierloot, K.; Vancoillie, S. Relative energy of the high-($^5T_{2g}$) and low-($^1A_{1g}$) spin states of $[Fe(H_2O)_6]^{2+}$, $[Fe(NH_3)_6]^{2+}$, and $[Fe(bpy)_3]^{2+}$: CASPT2 versus density functional theory. *J. Chem. Phys*., **2006**, *125*, 124303.

[174] te Velde, G.; Bickelhaupt, F.M.; Baerends, E.J.; Fonseca Guerra, C.; van Gisbergen, S.J. A.; Snijders, J.G.; Ziegler, T. Chemistry with ADF. *J. Comput. Chem.,* **2001**, *22*, 931-967.

[175] Bickelhaupt, F.M.; Baerends, E.J. Kohn-Sham DFT: Predicting and Understanding Chemistry. *Rev. Comput. Chem.,* **2000**, *15*, 1-86.

[176] Kitaura, K.; Morokuma, K. A new energy decomposition scheme for molecular interactions within the Hartree-Fock approximation. *Int. J. Quantum Chem.,* **1976**, *10*, 325-340.

[177] Ziegler, T.; Rauk, A. On the Calculation of Bonding Energies by the Hartree Fock Slater method. I. The Transition State Method. *Theoret. Chim. Acta,* **1978**, *46*, 1-10.

[178] Frenking, G.; Fröhlich, N. The Nature of the Bonding in Transition-Metal Compounds. *Chem. Rev.* **2000**, *100*, 717-774.

[179] Sato, T.; Sugao, K.; Oumi, Y.; Vetrivel, R.; Chatterjee, M.; Chatterjee, A.; Kubo, M.; Stirling, A.; Fahmi, A.; Miyamoto, A. Molecular dynamics simulation of metal porphyrin complex encapsulated in zeolite. *Appl. Surf. Sci.,* **1997**, *119*, 346-350.

[180] Zhan, B.-Z.; Li, X.-Y. A novel 'build-bottle-around-ship' method to encapsulate metalloporphyrins in zeolite-Y. An efficient biomimetic catalyst. *Chem. Commun.,* **1998**, 349-350.

[181] Moghadam, M.; Tangestaninejad, S.; Mirkhani, V.; Mohammadpoor-Baltork, I.; Moosavifar, M. Host (nanocavity of zeolite-Y or X)-guest (manganese (III) tetrakis[4-N-methylpyridinum]porphyrin) nanocomposite materials as efficient catalysts for biomimetic alkene epoxidation with sodium periodate: Shape-selective epoxidation of linear alkenes. *J. Mol. Catal. A*: *Chem.,* **2009**, *302*, 68-75.

[182] Alkordi, M.H.; Liu, Y.; Larsen, R.W.; Eubank, J.F.; Eddaoudi, M. Zeolite-like Metal-Organic Frameworks as Platforms for Applications: On Metalloporphyrin-Based Catalysts. *J. Am. Chem. Soc.,* **2008**, *130*, 12639-12641.

[183] Zhang, Z.; Zhang, L.; Wojtas, L.; Nugent, P.; Eddaoudi, M.; Zaworotko, M.J. Templated Synthesis, Postsynthetic Metal Exchange, and Properties of a Porphyrin-Encapsulating Metal-Organic Material. *J. Am. Chem., Soc.* **2012**, 924-927.

[184] Seidel, S.R.; Stang, P.J. High-Symmetry Coordination Cages via Self-Assembly. *Acc. Chem. Res.* **2002**, *35*, 972-983.

[185] Fujita, M.; Tominaga, M.; Hori, A.; Therrien, B. Coordination Assemblies from a Pd(II)-Cornered Square Complex. *Acc. Chem. Res.,* **2005**, *38*, 369-378.

[186] Yoshizawa, M.; Fujita, M. Self-assembled coordination cage as a molecular flask. *Pure Appl. Chem*., **2005**, *77*, 1107-1112.

[187] Ward, M.D. Polynuclear coordination cages. *Chem. Commun.* **2009**, 4487-4499.

[188] Ono, K.; Yoshizawa, M.; Akita, M.; Kato, T.; Tsunobuchi, Y.; Ohkoshi, S.-I.; Fujita, M. Spin Crossover by Encapsulation. *J. Am. Chem. Soc.,* **2009**, *131*, 2782-2783.

[189] Bader, R.F. W. Atoms in molecules: a quantum theory; The international series of monographs on chemistry; *Oxford University Press: Oxford, England*, **1994**; Vol. *22*.

[190] Matta, C.F., Boyd, R.J., Eds. The Quantum Theory of Atoms in Molecules; Wiley-VCH Verlag: Weinheim, **2007**.

[191] Becke, A.D.; Edgecombe, K.E. A simple measure of electron localization in atomic and molecular systems. *J. Chem. Phys.* **1990**, *92*, 5397-5403.

[192] Savin, A.; Becke, A.D.; Flad, J.; Nesper, R.; Preuss, H.; von Schnering, H.G. A New Look at Electron Localization. *Angew. Chem. Int.,* Ed. **1991**, *30*, 409-412.

[193] Savin, A.; Jepsen, O.; Flad, J.; Andersen, O.K.; Preuss, H.; von Schnering, H.G. Electron Localization in Solid-State Structures of the Elements: the Diamond Structure. *Angew. Chem. Int.,* Ed. **1992**, *31*, 187-188.

[194] Savin, A.; Nesper, R.; Wengert, S.; Fässler, T.F. ELF: The Electron Localization Function. *Angew. Chem. Int.,* Ed. **1997**, *31*, 1808-1832.

[195] Kohout, M.; Pernal, K.; Wagner, F.R.; Grin, Y. Electron localizability indicator for correlated wavefunctions.I. Parallel-spin pairs. *Theor. Chem. Acc.,* **2004**, *112*, 453-459.

[196] Kohout, M. A Measure of Electron Localizability. *Int. J. Quantum Chem.* **2004**, *97*, 651-658.

[197] Wagner, F.R.; Bezugly, V.; Kohout, M.; Grin, Y. Charge Decomposition Analysis of the Electron Localizability Indicator: A Bridge between the Orbital and Direct Space Representation of the Chemical Bond. *Chem. Eur. J.,* **2007**, *13*, 5724-5741.

[198] Marzari, N.; Mostofi, A.A.; Yates, J.R.; Souza, I.; Vanderbilt, D. Maximally localized Wannier functions: Theory and applications. *Rev. Mod. Phys.,* **2012**, *85*, 1419-1475.

[199] Chumakov, Y.; Matouzenko, G.S.; Borshch, S.A.; Postnikov, A. Quantum chemical studies of spin crossover polymers: Periodic DFT approach. *Polyhedron,* **2009**, *28*, 1955-1957.

[200] Garcia, Y.; Niel, V.; Munoz, M.C.; Real, J.A. Spin crossover in 1D, 2D and 3D polymeric Fe(II) networks. *Top. Curr. Chem.,* **2004**, *233*, 229-257.

[201] Lemercier, G.; Bréfuel, N.; Shova, S.; Wolny, J.A.; Dahan, F.; Verelst, M.; Paulsen, H.; Trautwein, A.X.; Tuchagues, J.-P. A Range of Spin-Crossover Temperature $T_{1/2}$>300 K Results from Out-of-Sphere Anion Exchange in a Series of Ferrous Materials Based on the 4-(4-Imidazolylmethyl)-2-(2-imidazolylmethyl)imidazole (trim) Ligand, $(Fe(trim)_2)X_2$ (X=F, Cl, Br, I): Comparison of Experimental Results with Those Derived from Density Functional Theory Calculations. *Chem. Eur. J*., **2006**, *12*, 7421-7432.

[202] Lebègue, S.; Pillet, S.; Ángyán, J.G. Modeling spin-crossover compounds by periodic DFT + U approach. *Phys. Rev. B,* **2008**, *78*, 024433.

[203] Sarkar, S.; Tarafder, K.; Oppeneer, P.M.; Saha-Dasgupta, T. Spin-crossover in cyanide-based bimetallic coordination polymers-insight from first-principles calculations. *J. Mater. Chem.,* **2011**, *21*, 13832-13840.

[204] Bučko, T.; Hafner, J.; Lebègue, S.; Ángyán, J.G. Spin crossover transition of $Fe(phen)_2(NCS)_2$: periodic dispersion-corrected density-functional study. P*hys. Chem. Chem. Phys.,* **2012**, 5389-5396.

[205] Tarafder, K.; Kanungo, S.; Oppeneer, P.M.; Saha-Dasgupta, T. Pressure and Temperature Control of Spin-Switchable Metal-Organic Coordination Polymers from *Ab Initio* Calculations. *Phys. Rev. Lett*., **2012**, *109*, 077203.

[206] Kowalski, K.; Valiev, M. Extensive regularization of the coupled cluster methods based on the generating functional formalism: Application to gas-phase benchmarks and to the S_N2 reaction of $CHCl_3$ and OH^- in water. *J. Chem. Phys.*, **2009**, *131*, 234107.

[207] Bartlett, R.J.; Musiał, M. Coupled-cluster theory in quantum chemistry. *Rev. Mod. Phys*., **2007**, *79*, 291-352.

[208] Krylov, A.I. Equation-of-Motion Coupled-Cluster Methods for Open-Shell and Electronically Excited Species: The Hitchhiker's Guide to Fock Space. *Annu. Rev. Phys. Chem*., **2008**, *59*, 433-462.

[209] Zheng, J.; Gour, J.R.; Lutz, J.J.; Piecuch, M.W.P.; Truhlar, D.G. A comparative assessment of the perturbative and renormalized coupled cluster theories with a noniterative treatment of triple excitations for thermochemical kinetics, including a study of basis set and core correlation effects. *J. Chem. Phys.,* **2008**, *128*, 044108.

[210] Raghavachari, K.; Trucks, G.W.; Pople, J.A.; Head-Gordon, M. A fifth-order perturbation comparison of electron correlation theories. *Chem. Phys. Lett.,* **1989**, *157*, 479-483.

[211] Lawson Daku, L.M.; Aquilante, F.; Robinson, T.W.; Hauser, A. Accurate Spin-State Energetics of Transition Metal Complexes: I. CCSD(T), CASPT2 and DFT Study of $[M(NCH)_6]^{2+}$ (M =Fe, Co). *J. Chem. Theory Comput*., **2012**, *8*, 4216-4231.

[212] Andersson, K.; Malmqvist, P.-A.; Roos, B.O.; Sadlej, A.J.; Wolinski, K. Secondorder perturbation theory with a CASSCF reference function. *J. Phys. Chem*., **1990**, *94*, 5483-5488.

[213] Andersson, K.; Malmqvist, P.-A.; Roos, B.O. Second-order perturbation theory with a complete active space self-consistent field reference function. *J. Chem. Phys.,* **1992**, *96*, 1218-1226.

[214] Ma, S.-K.; Brueckner, K.E. Correlation Energy of an Electron Gas with a Slowly Varying High Density. *Phys. Rev.,* **1968**, *165*, 18-31.

[215] Langreth, D.C.; Mehl, M.J. Beyond the local-density approximation in calculations of ground-state electronic properties. *Phys. Rev. B,* **1983**, *28*, 1809-1834.

[216] Langreth, D.C.; Mehl, M.J. Erratum: Beyond the local-density approximation in calculations of ground-state electronic properties. *Phys. Rev. B,* **1984**, *29*, 2310.

[217] Perdew, J.P.; Kurth, S.; Zupan, A.; Blaha, P. Accurate Density Functional with Correct Formal Properties: A Step Beyond the Generalized Gradient Approximation. *Phys. Rev. Lett*., **1999**, *82*, 2544-2547.

[218] Perdew, J.P.; Kurth, S.; Zupan, A.; Blaha, P. Erratum: Accurate Density Functional with Correct Formal Properties: A Step Beyond the Generalized Gradient Approximation [*Phys. Rev. Lett.* 82, 2544 (**1999**)]. *Phys. Rev. Lett.,* **1999**, *82*, 5179.

[219] Nekovee, M.; Foulkes, W.M.C.; Needs, R.J. Quantum Monte Carlo Analysis of Exchange and Correlation in the Strongly Inhomogeneous Electron Gas. *Phys. Rev. Lett*. **2001**, *87*, 036401.

[220] Perdew, J.P.; Tao, J.; Staroverov, V.N.; Scuseria, G.E. Meta-generalized gradient approximation: Explanation of a realistic nonempirical density functional. *J. Chem. Phys.,* **2004**, *120*, 6898-6911.

[221] Becke, A.D. A new mixing of Hartree-Fock and local density-functional theories. *J. Chem. Phys.,* **1993**, *98*, 1372-1377.

[222] Becke, A.D. Density-functional thermochemistry. III. The role of exact exchange. *J. Chem. Phys.,* **1993**, *98*, 5648-5652.

[223] Savin, A. In Recent Advances in Density Functional Methods (Part I); Chong, D.P., Ed.; Recent Advances In Computational Chemistry; **1995**; Vol. *1*; pp 129-153.

[224] Leininger, T.; Stoll, H.; Werner, H.-J.; Savin, A. Combining long-range configuration interaction with short-range density functionals. *Chem. Phys. Lett.* **1997**, *275*, 151-160.

[225] Toulouse, J.; Colonna, F.; Savin, A. Long-range-short-range separation of the electron-electron interaction in density-functional theory. *Phys. Rev. A,* **2004**, *70*, 062505.

[226] Iikura, H.; Tsuneda, T.; Yanai, T.; Hirao, K. A long-range correction scheme for generalized-gradient-approximation exchange functionals. *J. Chem. Phys*., **2001**, *115*, 3540-3544.

[227] Tawada, Y.; Tsuneda, T.; Yanagisawa, S.; Yanai, T.; Hirao, K. A long-range-corrected time-dependent density functional theory *J. Chem. Phys*., **2004**, *120*, 8425-8433.

[228] Song, J.-W.; Hirosawa, T.; Tsuneda, T.; Hirao, K. Long-range corrected density functional calculations of chemical reactions: Redetermination of parameter. *J. Chem. Phys*., **2007**, *126*, 154105.

[229] Yanai, T.; Tew, D.P.; Handy, N.C. A new hybrid exchange-correlation functional using the Coulomb-attenuating method (CAM-B3LYP). *Chem. Phys*. Lett., **2004**, *393*, 51-57.

[230] Rohrdanz, M.A.; Herbert, J.M. Simultaneous benchmarking of ground- and excited-state properties with long-range-corrected density functional theory. *J. Chem. Phys*., **2008**, *129*, 034107.

[231] Grimme, S. Semiempirical hybrid density functional with perturbative second-order correlation. *J. Chem. Phys*., **2006**, *124*, 034108.

[232] Schwabe, T.; Grimme, S. Towards chemical accuracy for the thermodynamics of large molecules: new hybrid density functionals including non-local correlation effects. *Phys. Chem. Chem. Phys*. **2007**, *8*, 4398-4401.

[233] Schwabe, T.; Grimme, S. Theoretical Thermodynamics for Large Molecules: Walking the Thin Line between Accuracy and Computational Cost. *Acc. Chem. Res*., **2008**, *41*, 569-579.

[234] Ghigo, G.; Roos, B.O.; Malmqvist, P.-A. A modified definition of the zeroth-order Hamiltonian in multiconfigurational perturbation theory (CASPT2). *Chem. Phys. Lett*., **2004**, *396*, 142-149.

[235] Suaud, N.; Bonnet, M.-L.; Boilleau, C.; Labèguerie, P.; Guihéry, N. Light-Induced Excited Spin State Trapping: Ab Initio Study of the Physics at the Molecular Level. *J. Am. Chem. Soc*. **2009**, *131*, 715-722.

[236] Kepenekian, M.; Robert, V.; Le Guennic, B. What zeroth-order Hamiltonian for CASPT2 adiabatic energetics of $Fe(II)N_6$ architectures? *J. Chem. Phys*., **2009**, *131*, 114702.

[237] Xu, X.; Goddard III, W.A. The X3LYP extended density functional for accurate descriptions of nonbond interactions, spin states, and thermochemical properties. *Proc. Natl. Acad. Sci. U.S.A*., **2004**, *101*, 2673-2677.

[238] Zhao, Y.; Truhlar, D.G. The M06 suite of density functionals for main group thermochemistry, thermochemical kinetics, noncovalent interactions, excited states, and transition elements: two new functionals and systematic testing of four M06-class functionals and 12 other functionals. *Theor. Chem. Acc.,* **2008**, *120*, 215-241.

[239] Vargas, A.; Krivokapic, I.; Hauser, A.; Lawson Daku, L.M. Towards accurate estimates of the spin-state energetics of spin-crossover complexes within density functional theory: a comparative case study of cobalt(II) complexes. *Phys. Chem. Chem. Phys*., **2013**, *15*, 3752-3763.

[240] Mizuno, K.; Lunsford, J.H. Electron paramagnetic resonance study of tris(2,2'-bipyridine)cobalt(II) complexes in zeolite Y: evidence for spin equilibrium. *Inorg. Chem*., **1983**, *22*, 3484-3486.

[241] Tiwary, S.K.; Vasudevan, S. Spin crossover in the ship-in-a-bottle compound: cobalt(II)tris(bipyridyl) encapsulated in zeolite-Y. *Chem. Phys. Lett*., **1997**, *277*, 84-88.

[242] Tiwary, S.K.; Vasudevan, S. Void Geometry Driven Spin Crossover in Zeolite-Encapsulated Cobalt Tris(bipyridyl) Complex Ion. *Inorg. Chem*., **1998**, *37*, 5239-5246.

[243] Sieber, R.; Decurtins, S.; Stoeckli-Evans, H.; Wilson, C.; Yufit, D.; Howard, J.A.K.; Capelli, S.C.; Hauser, A. A Thermal Spin Transition in $[Co(bpy)_3][LiCr(ox)_3]$ (ox = $C_2O_4^{2-}$) ; bpy =2,2'-bipyridine. *Chem. Eur. J*., **2000**, *6*, 361-368.

[244] Zerara, M.; Hauser, A. Cobalt(II)-tris-2,2'-bipyridine as a Spin-Crossover Complex: Evidence for Cooperative Effects in Three-Dimensional Oxalate Networks. *ChemPhysChem,* **2004**, *5*, 395-399.

[245] Hogg, R.; Wilkins, R.G. Exchange studies of certain chelate compounds of the transitional metals. Part VIII. 2,2',2"-terpyridine complexes. *J. Chem. Soc*., **1962**, *341*-350.

[246] Stoufer, R.C.; Smith, D.W.; Clevenger, E.A.; Norris, T.E. Complexes of Cobalt(II). I. On the Anomalous Magnetic Behavior of Some Six-Coordinate Cobalt(II) Complexes. *Inorg. Chem*., **1966**, *5*, 1167-1171.

[247] Judge, J.S.; Baker Jr., W.A. On the spin equilibrium in bis(2,2':6',2"-terpyridine) cobalt(II) salts. *Inorg. Chim. Acta,* **1967**, *1*, 68-72.

[248] Schmidt, J.G.; Brey Jr., W.S.; Stoufer, R.C. Complexes of Cobalt(II). IV. On the Electron Paramagnetic Resonance Spectra of Some Magnetically Anomalous Complexes of Cobalt(II). *Inorg. Chem*. **1967**, *6*, 268-271.

[249] Harris, C.M.; Lockyer, T.N.; Martin, R.L.; Patil, H.R.H.; Sinn, E. Five- and six-coordinated complexes of cobalt(II) with 2,2',2'-terpyridyl: Unusual structure and magnetism. *Aust. J. Chem*., **1969**, *22*, 2105-2116.

[250] Maslen, E.N.; Raston, C.L.; White, A.H. Crystal structure of bis-(2,2':6',2"-terpyridyl)cobalt(II) bromide trihydrate. *J. Chem. Soc*., Dalton Trans. **1974**, 1803-1807.

[251] Raston, C.L.; White, A.H. Crystal structures of bis(terpyridyl) cobalt(II) thiocyanate dihydrate: an X-ray-induced phase transition? *J. Chem. Soc*., Dalton Trans. **1976**, 7-12.

[252] Henke, W.; Kremer, S. The crystal structure of high-spin low-spin bis(2.2':6'2"- terpyridyl) Co(II) perchlorate. *Inorg. Chim. Acta,* **1982**, *65*, L115-L117.

[253] Kremer, S.; Henke, W.; Reinen, D. High-Spin-Low-Spin Equilibria of Cobalt(2+) in the Terpyridine Complexes $Co(terpy)_2X_2 \cdot nH_2O$. *Inorg. Chem*., **1982**, *21*, 3013-3022.

[254] Figgis, B.N.; Kucharski, E.S.; White, A.H. Crystal Structure of Bis(2,2':6',2"- terpyridyl)cobalt(II) Iodide Dihydrate at 295 K and at 120 K. Aust. *J. Chem*. **1983**, *36*, 1527-1535.

[255] Figgis, B.N.; Kucharski, E.S.; White, A.H. Crystal Structure of Bis(2,2':6',2"- terpyridyl)cobalt(II) Perchlorate c. 1.3 Hydrate. Aust. *J. Chem*., **1983**, *36*, 1537-1561.

[256] Beattie, J.K.; Binstead, R.A.; Kelso, M.T.; Favero, P.D.; Dewey, T.G.; Turner, D.H. Dynamics of cobalt(II) spin-equilibrium complexes. *Inorg. Chim. Acta,* **1995**, *235*, 245-251.

[257] Enachescu, C.; Krivokapic, I.; Zerara, M.; Real, J.A.; Amstutz, N.; Hauser, A. Optical investigation of spin-crossover in cobalt(II) bisterpy complexes. *Inorg. Chim. Acta,* **2007**, *360*, 3945-3950.

[258] Krivokapic, I.; Zerara, M.; Lawson Daku, L.M.; Vargas, A.; Enachescu, C.; Ambrus, C.; Tregenna-Piggott, P.; Amstutz, N.; Krausz, E.; Hauser, A. Spin-crossover in cobalt(II) imine complexes. *Coord. Chem. Rev*., **2007**, *251*, 364-378.

Received: November 10, 2013 **Revised: December 02, 2013** **Accepted: December 02, 2013**